Journal of Inorganic Biochemistry 127 (2013) 188–202

Contents lists available at ScienceDirect

Journal of Inorganic Biochemistry

journal homepage: www.elsevier.com/locate/jinorgbio

New bifunctional metalloproteinase inhibitors: an integrated approach towards biological improvements and cancer therapy

Sérgio M. Marques [a], Claudia C. Abate [a,b], Sílvia Chaves [a], Fernanda Marques [c], Isabel Santos [c], Elisa Nuti [b], Armando Rossello [b], M. Amélia Santos [a,*]

[a] Centro de Química Estrutural, Instituto Superior Técnico, Universidade Técnica de Lisboa, Av. Rovisco Pais 1, 1049-001 Lisboa, Portugal
[b] Dipartimento di Farmacia, Università di Pisa, Via Bonanno 6, 56126 Pisa, Italy
[c] IST/ITN, Instituto Superior Técnico, Universidade Técnica de Lisboa, Estrada Nacional Nº 10, 2686-953 Sacavém, Portugal

ARTICLE INFO

Article history:
Received 18 December 2012
Received in revised form 5 March 2013
Accepted 6 March 2013
Available online 16 March 2013

Keywords:
Metalloproteinase inhibitors
MMPs zinc-binding groups
Hydrazide derivatives
Stability constants
Benzothiazole

ABSTRACT

The key role of some matrix metalloproteinases (MMPs) on several pathological processes, including carcinogenesis and tumor growth, makes the development of MMP inhibitors (MMPIs) an attractive approach for cancer therapy. We present herein an integrated approach for the development of a new series of inhibitors of MMP2 and MMP14, two enzymes over-expressed by human ovarian cancer. As a first step, a new series of single model compounds bearing different zinc-binding groups (ZBGs), such as carboxylic, hydroxamic acid, hydrazide and sulfonylhydrazide groups, were studied and revealed reasonably good capacity for the Zn(II) chelation in solution and for the MMP inhibition. Aimed at further reinforcing the biological activity of these MMPIs as anti-cancer agents, a selection of those models was extra-functionalized with benzothiazole (BTA), a group with recognized antitumor activity. Analysis of the results obtained for these bifunctional compounds, in particular the inhibitory activity against MMP2 and MMP14 as well as the anti-proliferative activity on the A2780 ovarian cancer cell line, allowed to understand the activity dependence on the type of ZBG, as well as the relevance of the BTA moiety. Overall, the evidenced BTA-associated activity improvements on enzyme inhibition and cell antiproliferactivity, combined with the hydrolytic stability revealed by the hydrazide group, suggest that these new bifunctional BTA-hydrazide derivatives should be taken in consideration for the development of new generations of MMPIs with anti-cancer activity.

1. Introduction

Matrix metalloproteinases (MMPs) are a family of zinc-dependent proteases responsible for degradation of several extracellular matrix components. In normal conditions, they play important physiological roles, such as in tissue remodeling, cellular homeostasis and innate immunity control. However, when dysregulated, they become the cause of many pathological processes, such as arthritis, osteoarthritis, chronic inflammation, angiogenesis and cancer [1,2]. In particular, MMP2 and MMP14 play a key role in several types of carcinomes, such as the human ovarian carcinoma, being over-expressed by the corresponding cancer cells [3]. Both enzymes degrade collagens very effectively and in similar manners, in spite of having different domain organizations and belonging to different subgroups: gelatinase (MPP2) and membrane-type (MMP14) [4]. MMPs have been an attractive pharmaceutical target, namely through the development of MMP inhibitors (MMPIs) for several pathologies, including cancer [5,6]. The great majority of MMPIs enclose a zinc-binding group (ZBG) to interact with the catalytic zinc ion at the enzyme active site. Most of the MMPIs so far developed contain a hydroxamic acid (HA) as ZBG, because of its great ability to bind Zn(II) and specific amino acid residues at the active site of the MMPs (e.g. CGS 27023A, Fig. 1). However, this functional group is known for presenting pharmacokinetic drawbacks associated with its hydrolytic lability, which may account for failures of those inhibitors in clinical trials [7].

Thus, the design of new MMPI generations with major changes in the Zn(II) chelating groups has been a recent challenge for several research groups, including ours [8–10]. In particular, we have recently embarked on the development of new series of MMPIs, with backbones identical to other previously reported hydroxamic-based sulfonylated MMP inhibitors [9], but bearing different ZBGs, namely hydroxypyrimidinone [11] and 1-hydroxypiperazine-2,6-diones [12].

However, the question still remains: working on targeting Zn(II) ion, is it a suitable way to inhibit MMPs? To step forward on that purpose, several features must be taken into account, namely structural, steric and electronic considerations. Concerning the Zn(II) ion, since it is a borderline Lewis acid (between the hard and the soft ones), it can interact with a variety of donor atoms, including sulfur, nitrogen and also oxygen. The effectiveness and selectivity of a Zn-chelating drug

* Corresponding author. Tel.: +351 218419273, +351 218419301; fax: +351 218464455.
E-mail address: masantos@ist.utl.pt (M.A. Santos).

0162-0134/$ – see front matter © 2013 Elsevier Inc. All rights reserved.
http://dx.doi.org/10.1016/j.jinorgbio.2013.03.003

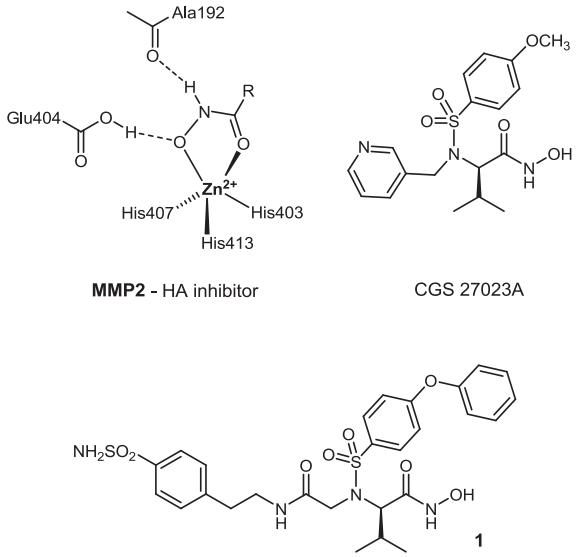

Fig. 1. Binding mode of a general HA-based inhibitor within the catalytic site of MMP2, and two HA-based inhibitors: the broad spectrum CGS 27023A [2] and the MMP/carbonic anhydrase dual target inhibitor **1** [9].

are, at least partly, related to its thermodynamic ability to coordinate the metal ions and to compete with the biological ligands that bind to the cofactor in its enzymatic environment.

Herein, we present an integrated approach towards the development of a new series of MMP2 and MMP14 inhibitors. The starting hallmark is a set of simple MMPI models, containing an *N*-sulfonylaryl moiety in the main skeleton and different ZBGs, such as carboxylic acid, HA, hydrazide, sulfonylhydrazide and hydrazone. The physical–chemical properties of a representative group of these model compounds are assessed, such as the Zn(II)-binding affinity and the coordination mode. Furthermore, to pursuit our interest on developing polyfunctional drug candidates for cancer therapy (e.g. compound **1**, Fig. 1 [9]), we have decided to further explore the influence that an extrafunctional benzothiazole (BTA) group, known for its biological activity as anticancer [13–15], could have on the biological activity of these MMPIs.

Therefore, we describe herein the preparation of the new set of *N*-sulfonated MMP inhibitors bearing different ZBG, either as simple truncated models or as dual targeting BTA-containing MMPIs. The results of solution equilibrium Zn(II)-complexation studies and of bioassessing the inhibitory activity against MMP2 and 14, as well as the anti-tumor activity against A2780 human ovarian carcinoma cells, are also presented. In silico studies of the ligand-protein binding interactions were also performed aimed at shedding some light on the rationalization of the enzymatic activity. A comparative analysis of the results is mostly focused on the effect of different ZBGs and of the presence of the BTA extra-functional group on the biological activities, although the effect of linkers and hydrolytic stability is also considered. These results may offer new insights for consideration in cancer treatment strategies.

2. Experimental

2.1. Materials and methods

Analytical grade reagents were purchased from Aldrich, Sigma and Fluka and were used as supplied. Solvents were dried according to standard methods [16]. The chemical reactions were monitored by thin layer chromatography (TLC) using alumina plates coated with silica gel 60 F_{254} (Merck). Column flash chromatography separations were performed on silica gel Merck 230–400 mesh ASTM. Melting points were measured with a Leica Galen III hot stage apparatus and are uncorrected. The NMR spectra were measured on Bruker AVANCE III 300 MHz and Bruker AVANCE III 400 MHz spectrometers, at 25 °C. Chemical shifts (δ) are reported in ppm, from standard internal references, namely tetramethylsilane (TMS) for organic solvents and sodium 3-(trimethylsilyl)-[2,2,3,3-d4]-propionate (DSS) for D_2O solutions. The following abbreviations are used: s = singlet, d = doublet, t = triplet, qd = quadruplet, qt = quintuplet, m = multiplet, dd = double doublet,Ł and bs = broad singlet. Peak attribution was, whenever necessary, confirmed by two-dimensional NMR experiments, namely correlation spectroscopy (COSY) and heteronuclear single quantum coherence spectroscopy (HSQC). The electrospray ionization mass spectra (ESI MS) were obtained on a 500 MS LC Ion Trap (Varian Inc., Palo Alto, CA, USA) mass spectrometer equipped with an ESI ion source, operated in the positive or negative ion mode.

2.2. Synthesis of the compounds

2.2.1. Ethyl 2-(4-phenoxyphenylsulfonamido)acetate (**2m**)

A mixture of glycine ethyl ester hydrochloride (1.72 g, 12.3 mmol), 4-phenoxybenzenesulfonyl chloride, prepared as previously reported [17] (3.02 g, 11.2 mmol), and triethylamine (2.7 mL, 24.6 mmol) in CH_3CN (50 mL) was stirred at r.t. for 1 day. The mixture was then filtered and the solvent evaporated. The final residue was dissolved in Et_2O (75 mL) and subsequently washed with 0.1 M HCl (2 × 75 mL) and 5% NaOH (2 × 75 mL) solutions and also with H_2O (75 mL). The final organic phase was dried over anhydrous Na_2SO_4, and the solvent evaporated to afford the pure compound as a pale beige solid (3.20 g, 85% yield), m.p. 68–71 °C. ^{1}H NMR (CDCl3), δ (ppm): 7.81 (d, J = 9.0 Hz, 2H, PhOPh**H**), 7.40 (t, J = 7.5 Hz, 2H, PhOPh**H**), 7.24 (t, J = 7.5 Hz, 1H, PhOPh**H**), 7.07–7.02 (m, J = 7.5 Hz, 4H, PhOPh**H**), 5.07 (t, J = 4.5 Hz, 1H, N**H**), 4.12 (qd, J = 8.0 Hz, 2H, C**H**$_2$CH$_3$), 3.78 (d, J = 6.0 Hz, 2H, C**H**$_2$NH), 1.21 (t, J = 7.5 Hz, 3H, CH$_2$C**H**$_3$); m/z (ESI MS): 336.0 $(M + H)^+$, 358.1 $(M + Na)^+$.

2.2.2. 2-(4-Phenoxyphenylsulfonamido)acetic acid (**2a**)

To a solution of **2m** (2.02 g, 6.02 mmol) in MeOH (20 mL) was added 2 M KOH (2 mL) and the mixture was stirred at r.t. for 4 h. The final solution was evaporated and 5% NaOH (75 mL) was added to the residue, and then the resulting solution was washed with CH_2Cl_2 (4 × 50 mL). The aqueous phase was acidified with conc. HCl until precipitation occurred and the mixture was extracted with EtOAc (3 × 50 mL). The total organic phase was washed with H_2O (2 × 50 mL), dried over anhydrous Na_2SO_4, and the solvent was evaporated. After recrystallization from MeOH/Et_2O, the pure product was obtained as a white solid (1.71 g, 92% yield), m.p. 167–169 °C. ^{1}H NMR (DMSO-d6), δ (ppm): 7.98 (t, J = 6.0 Hz, 1H, N**H**), 7.78 (d, J =8.6 Hz, 2H, PhOPh**H**), 7.46 (t, J = 7.6 Hz, 2H, PhOPh**H**), 7.25 (t, J =7.3 Hz, 1H, PhOPh**H**), 7.14–7.08 (m, 4H, PhOPh**H**), 3.57 (d, J =5.9 Hz, 2H, C**H**$_2$); m/z (ESI MS): 330.0 $(M + Na)^+$, 306.1 $(M-H)^-$.

2.2.3. N-(benzyloxy)-2-(4-phenoxyphenylsulfonamido)acetamide (**2bp**)

Two different methods were used for the carboxylic acid-amine coupling to form the amide bonds. They differ mostly in the carboxylic activation reagents and reaction time, and, in certain cases, one was preferable over the other one. Below are described the two methods applied on the synthesis of **2bp**.

2.3. Method A

To a solution of **2a** (0.220 g, 0.716 mmol), *O*-benzylhydroxylamine hydrochloride (0.114 g, 0.716 mmol), and *N*-methylmorpholine (NMM, 0.28 mL, 2.51 mmol) in 9:1 CH_2Cl_2/EtOAc (10 mL) was added dropwise a solution 50% propylphosphonic anhydride (T3P) in EtOAc (0.46 mL,

0.86 mmol), and the mixture was stirred at r.t. for 2 h. The solvent was then evaporated and the crude material was taken into EtOAc (25 mL) and this solution was successively washed with H_2O (25 mL), 0.1 M HCl (3 × 25 mL), 0.1 M NaOH (2 × 25 mL) and H_2O (2 × 25 mL). The resulting organic phase was dried over anhydrous Na_2SO_4, filtered and the solvent was evaporated, affording the pure product as a beige solid (0.224 g, 76% yield).

2.4. Method B

To a solution of **2a** (0.200 g, 0.651 mmol), 1-ethyl-3-(3-dimethylaminopropyl) carbodiimide hydrochloride (EDC.HCl, 0.150 g, 0.781 mmol) and 4-dimethylaminopyridine (DMAP, 8 mg, 0.065 mmol) in CH_2Cl_2 (30 mL) was added *O*-benzylhydroxylamine hydrochloride (0.125 g; 0.781 mmol) and *N*-methylmorpholine (NMM, 0.086 mL, 0.781 mmol), and the mixture was stirred at room temperature (r.t.) for 16 h. The final solution was evaporated, dissolved in EtOAc (25 mL) and washed with 0.1 M HCl (3 × 25 mL), 0.1 M NaOH (2 × 25 mL) and then H_2O (1 × 25 mL). The final organic phase was dried over anhydrous Na_2SO_4, and the solvent evaporated. The crude was recrystallized from Et_2O/n-hexane, affording the pure compound as white solid (0.180 g; 67% yield), m.p. 106–108 °C. ^{1}H NMR (MeOD), δ (ppm): 7.76 (d, J = 8.4 Hz, 2H, PhOPh**H**), 7.36–7.25 (m, 7H, PhOPh**H**, Ph**H**), 7.15 (t, J = 7.4 Hz, 1H, PhOPh**H**), 7.03–6.98 (m, 4H, PhOPh**H**), 4.66 (s, 2H, C**H**$_2$Ph), 3.43 (s, 2H, NHC**H**$_2$CO); m/z (ESI MS): 413.0 $(M + H)^+$, 435.0 $(M + Na)^+$.

2.4.1. N-hydroxy-2-(4-phenoxyphenylsulfonamido)acetamide (2b)

The standard method for catalytic hydrogenation was followed: a mixture of **2bp** (0.230 g, 0.558 mmol) and 5% Pd/C (0.050 g) in MeOH (10 mL) under 1.5 bar of H_2 was stirred at r.t. for 1 h. The mixture was then filtered and the liquid evaporated. Recrystallization of the crude material with ethyl ether afforded the pure product as a beige solid (0.150 g, 83% yield), m.p. 110–112 °C. ^{1}H NMR ($CDCl_3$, 5% MeOD), δ (ppm): 7.73 (d, J = 8.8 Hz, 2H, PhOPh**H**), 7.37 (t, J = 7.8 Hz, 2H, PhOPh**H**), 7.18 (t, J = 7.2 Hz, 1H, PhOPh**H**), 7.03–6.98 (m, 4H, PhOPh**H**), 3.49 (s, 2H, C**H**$_2$); m/z (ESI MS): 323.1 $(M + H)^+$, 345.1 $(M + Na)^+$.

2.4.2. N-(2-hydrazinyl-2-oxoethyl)-4-phenoxybenzenesulfonamide (2c)

A solution of **2m** (0.184 g, 0.549 mmol) and hydrazine hydrate (1 mL, 20 mmol) in ethanol (5 mL) was stirred overnight at r.t. The organic solvent was evaporated and, upon addition of cold water, a precipitate was formed. It was filtered and washed with small portions of cold water, and then with Et_2O to yield the pure product as a white solid (0.109 g, 62% yield), m.p. 114–115 °C. ^{1}H NMR (DMSO-d6), δ (ppm): 9.04 (s, 1H, CON**H**NH$_2$), 7.85 (bs, 1H, SO$_2$N**H**), 7.78 (d, J = 8.4 Hz, 2H, PhOPh**H**), 7.47 (t, J = 7.6 Hz, 2H, PhOPh**H**), 7.25 (t, J = 7.2 Hz, 1H, PhOPh**H**), 7.14–7.09 (m, 4H, PhOPh**H**), 4.24 (bs, 2H, CONHN**H**$_2$), 3.38 (s, 2H, C**H**2); m/z (ESI MS): 322.1 $(M + H)^+$, 344.1 $(M + Na)^+$.

2.4.3. 4-methoxybenzenesulfonylhydrazide

A solution of 4-methoxybenzenesulfonyl chloride (0.41 g, 1.98 mmol) and hydrazine hydrate (0.5 mL, 10.3 mmol) in CH_3CN (20 mL) was stirred for 1 h at r.t. The solvent was evaporated, the residue was taken in EtOAc (50 mL) and then the solution was sequentially washed with 0.1 M HCl (3 × 50 mL), 0.1 M NaOH (2 × 50 mL) and H_2O (2 × 50 mL). After drying the organic layer over anhydrous Na_2SO_4 and evaporating the solvent, the residue was washed with n-hexane to give the title compound as a white solid (0.310 g, 77% yield), m.p. 96–98 °C. ^{1}H NMR (DMSO-d6), δ (ppm): 8.19 (t, J = 3.2 Hz, 1H, SO$_2$N**H**NH$_2$), 7.72 (d, J = 8.7 Hz, 2H, Ph**H**), 7.12 (d, J =9.0, 2H, Ph**H**), 4.01 (d, J = 3.3 Hz, 2H, SO$_2$NHN**H**$_2$), 3.84 (s, 3H, OC**H**3); m/z (ESI MS): 203.1 $(M + H)^+$, 225.0 $(M + Na)^+$.

2.4.4. N-(2-(2-(4-methoxyphenylsulfonyl)hydrazinyl)-2-oxoethyl)-4-phenoxybenzenesulfonamide (2d)

Condensation of **2a** with 4-methoxybenzenesulfonylhydrazide was achieved following method A, as described in the synthesis of **2bp**. A white solid was obtained as the pure product (60% yield), m.p. 186–188 °C. ^{1}H NMR (DMSO-d6), δ (ppm): 9.99 (bs, 1H, CON**H**NHSO$_2$), 9.66 (bs, 1H, N**H**CH$_2$CO), 7.87 (bs, 1H, CONHN**H**SO$_2$), 7.78–7.68 (m, 4H, PhOPh**H**, Ph**H**), 7.47 (t, J = 7.1 Hz, 2H, PhOPh**H**), 7.25 (t, J = 6.9 Hz, 1H, PhOPh**H**), 7.14–7.03 (m, 6H, PhOPh**H**, Ph**H**), 3.82 (s, 3H, OC**H**$_3$), 3.42 (d, J = 5.6 Hz, 1H, NHC**H**$_2$CO); m/z (ESI MS): 514.0 $(M + Na)^+$, 490.0 $(M–H)^-$.

2.5. Procedure for the synthesis of the acylhydrazones 2e and 2g

2.5.1. N-(2-(2-(4-methoxybenzylidene)hydrazinyl)-2-oxoethyl)-4-phenoxybenzenesulfonamide (2e)

To a solution of **2c** (0.050 g, 0.156 mmol) in ethanol (5 mL) was added 4-anisaldehyde (20 μL, 0.16 mmol) and the mixture was stirred at 50 °C. After 30 min a white precipitate was formed; the reaction was left stirring for another 30 min, and afterwards it was left cool down in freezer for a few minutes. The solid was filtered off and washed with cold ethanol, to afford the pure title compound as a white solid (0.060 g, 88% yield), m.p. 203–204 °C. ^{1}H NMR (acetone-d6), δ (ppm): 7.97 (s, 1H, N = C**H**), 7.91 (d, J = 8.9 Hz, 2H, Ph**H**OCH$_3$), 7.64 (d, J = 8.7 Hz, 2H, PhOPh**H**), 7.45 (t, J = 8.0 Hz, 2H, PhOPh**H**), 7.24 (t, J = 7.4 Hz, 1H, PhOPh**H**), 7.13–6.98 (m, 4H, PhOPh**H**), 6.99 (d, J = 8.8 Hz, 2H, Ph**H**OCH$_3$), 4.20 (s, 2H, NHC**H**$_2$CO), 3.85 (s, 3H, OC**H**$_3$); m/z (ESI MS): 440.1 $(M + H)^+$, 462.1 $(M + Na)^+$.

2.5.2. N-(2-(2-(2-hydroxybenzylidene)hydrazinyl)-2-oxoethyl)-4-phenoxybenzenesulfonamide (2g)

Prepared by analogous procedure as for **2e**, but using salicylaldehyde instead of anisaldehyde; the final pure compound was obtained as white solid (82% yield), m.p. 177–179 °C. ^{1}H NMR (acetone-d6), δ (ppm): 8.45 (s, 1H, N = C**H**), 7.89 (d, J = 8.8 Hz, 2H, PhOPh**H**), 7.43 (t, J = 7.4 Hz, 2H, PhOPh**H**), 7.34–7.30 (m, 2H, Sal**H**), 7.23 (t, J = 7.4 Hz, 1H, PhOPh**H**), 7.11–7.05 (m, 4H, PhOPh**H**), 6.95–6.90 (m, 2H, Sal**H**), 3.78 (s, 2H, NHC**H**$_2$CO); m/z (ESI MS): 426.0 $(M + H)^+$, 447.9 $(M + Na)^+$.

2.5.3. N-(2-(2-(4-methoxybenzyl)hydrazinyl)-2-oxoethyl)-4-phenoxybenzenesulfonamide (2f)

To a solution of **2e** (0.030 g, 0.068 mmol) in acetic acid (1 mL) five portions of sodium borohydride (total of 0.025 g, 0.68 mmol) were added, in intervals of 15 min, and the mixture was stirred for 4 h. The reaction was quenched with MeOH, and when the gas release was over the solvent was evaporated under vacuum. The residue was washed with small portions of cold water, and then HCl-saturated MeOH solution was added until pH < 1. The solvent was evaporated and CH_3CN was added to the residue; the insoluble solid material was filtered and washed with cold CH_3CN, to afford the pure compound as a yellowish solid (0.012 g, 40% yield), m.p. 72–74 °C. ^{1}H NMR (MeOD), δ (ppm): 7.84 (d, J = 8.9 Hz, 2H, Ph**H**OCH$_3$), 7.45–7.40 (m, 4H, PhOPh**H**, Ph**H**OCH$_3$), 7.24 (t, J = 7.0 Hz, 1H, PhOPh**H**), 7.10–7.06 (m, 4H, PhOPh**H**), 7.00 (d, J = 8.7 Hz, 2H, Ph**H**OCH$_3$), 4.28 (s, 2H, NHC**H**$_2$PhOCH$_3$), 3.82 (s, 3H, OC**H**$_3$); 3.65 (s, 2H, NHC**H**$_2$CO); m/z (ESI MS): 464.0 $(M + Na)^+$, 440.0 $(M-H)^-$.

2.6. Synthesis and characterization of benzothiazole-amines (3 m–4 m)

2.6.1. Benzo[d]thiazol-2-ylmethanamine (3m)

A mixture of 2-aminothiophenol (ATP, 1.54 mL, 14.3 mmol) and glycine ethyl ester hydrochloride (2.0 g, 14.3 mmol) in polyphosphoric acid (10.0 g) was stirred at 220 °C for 4 h. The resulting brown oil was dissolved in 5 M NaOH (50 mL) to obtain a basic yellow solution, which was extracted with CH_2Cl_2 (2 × 30 mL). The total organic phase was

then extracted with 0.1 M HCl (2 × 30 mL), and afterwards it was washed with CH_2Cl_2 (50 mL). The aqueous phase was basified to pH ca. 10–12 with 5 M NaOH, and extracted with CH_2Cl_2 (2 × 30 mL). The total organic phase was dried over anhydrous Na_2SO_4, filtered and the solvent was evaporated. The brown oil obtained was acidified with HCl-saturated methanol until pH ca. 1, the solution was roto-evaporated, and the residue was recrystallized from CH_3CN, to afford the pure hydrochloric salt of the title compound as a beige solid (1.50 g, 52.3% yield), m.p. 183–186 °C. ^{1}H NMR (D_2O), δ (ppm): 8.11–8.08 (m, 2H, BTA**H**), 7.68–7.55 (m, 2H, BTA**H**), 4.73 (s, 2H, C**H**$_2$NH$_2$); m/z (ESI MS): 165.0 $(M + H)^+$.

*2.6.2. (R)-1-(benzo[d]thiazol-2-yl)-2-methylpropan-1-amine (**4m**)*

Analogous procedure as for **3m**, but D-valine was the starting material. The hydrochloric salt of the title compound was obtained as slightly hygroscopic beige solid (41% yield), m.p. 130–132 °C. ^{1}H NMR (D_2O), δ (ppm): 8.08–8.02 (m, 2H, BTA**H**), 7.58–7.50 (m, 2H, BTA**H**), 4.72 (d, J = 9.0 Hz, 1H, C**H**NH$_2$), 2.50–2.45 (m, 1H, C**H**$(CH_3)_2$), 1.14 (d, J = 6.0 Hz, 3H, C**H**$_3$), 0.99 (d, J = 9.0 Hz, 3H, C**H**$_3$); m/z (ESI MS): 207.1 $(M + H)^+$.

2.7. Synthesis and characterization of BTA-sulfonamides (3n–4n)

A method similar to the synthesis of **2m** was used, starting from compounds **3m–7m** but using 10% excess of phenoxybenzenesulfonyl chloride. Final recrystallization from n-hexane afforded the pure compounds.

*2.7.1. N-(benzo[d]thiazol-2-ylmethyl)-4-phenoxybenzenesulfonamide (**3n**)*

Pure compound as beige solid (99% yield), m.p. 133–135 °C. ^{1}H NMR (CDCl3), δ (ppm): 7.91 (d, J = 9.0 Hz, 1H, BTA**H**), 7.86–7.82 (m, 3H, BTA**H**, PhOPh**H**), 7.46–7.40 (m, 4H, BTA**H**, PhOPh**H**), 7.21 (t, J = 7.5 Hz, 1H, PhOPh**H**), 6.95 (d, J = 9.0 Hz, 4H, PhOPh**H**), 5.62 (t, J = 6.0 Hz, 1H, N**H**), 4.61 (d, J = 6.0 Hz, 2H, C**H**$_2$); m/z (ESI MS): 397.2 $(M + H)^+$.

*2.7.2. (R)-N-(1-(benzo[d]thiazol-2-yl)-2-methylpropyl)-4-phenoxybenzenesulfonamide (**4n**)*

After purification using flash chromatography (CH_2Cl_2 as eluent, R_f = 0.47), the pure compound was obtained as a light brown hygroscopic solid (50% yield). ^{1}H NMR ($CDCl_3$), δ (ppm): 7.86 (d, J =9.0 Hz, 1H, BTA**H**), 7.81 (d, J = 9.0 Hz, 1H, BTA**H**), 7.67 (d, J =9.0 Hz, 2H, PhOPh**H**), 7.48–7.42 (m, 4H, BTA**H**, PhOPh**H**), 7.16 (t, J = 7.5 Hz, 1H, PhOPh**H**), 6.70 (t, J = 7.5 Hz, 4H, PhOPh**H**), 5.62 (d, J = 9.0 Hz, 1H, N**H**), 4.55 (qd, J = 5.0 Hz, 1H, C**H**NH), 2.28–2.23 (m, 1H, C**H**$(CH_3)_2$), 1.03 (d, J = 9.0 Hz, 3H, C**H**$_3$), 0.95 (d, J = 6.0 Hz, 3H, C**H**$_3$); m/z (ESI MS): 439.2 $(M + H)^+$, 461.2 $(M + Na)^+$.

2.8. Synthesis and characterization of the tert-butyl acetate conjugates (3o–4o)

*2.8.1. Tert-butyl-2-(N-(benzo[d]thiazol-2-ylmethyl)-4-phenoxyphenylsulfonamido)acetate (**3o**)*

A suspension of **3n** (0.200 g, 0.50 mmol), K_2CO_3 (0.697 g, 2.52 mmol), KI (2.5 mg, 0.015 mmol) and *tert*-butyl 2-bromoacetate (0.11 mL, 0.75 mmol) in anhydrous DMF (15 mL) were stirred under nitrogen at r.t. for 3 days. Et_2O (15 mL) was added into the brown suspension and the total mixture was washed with H_2O (2 × 25 mL), 0.1 M HCl (2 × 15 mL), and H_2O again (25 mL). The final organic phase was dried over anhydrous Na_2SO_4, and the solvent was evaporated. The residue was washed several times with n-heptane, affording the pure product as a yellow oil, (0.290 g, 95% yield). ^{1}H NMR ($CDCl_3$), δ (ppm): 7.98 (d, J = 8.0 Hz, 1H, BTA**H**), 7.89–7.85 (m, 3H, BTA**H**, PhOPh**H**), 7.48–7.44 (m, 4H, BTA**H**, PhOPh**H**), 7.23 (t, J = 7.5 Hz, 1H, PhOPh**H**), 7.05–7.01 (m, 4H, PhOPh**H**), 4.95 (s, 2H, BTAC**H**$_2$), 4.10 (s, 2H, C**H**$_2$COO), 1.48 (s, 9H, *t*Bu**H**); m/z (ESI MS): 533.3 $(M + Na)^+$.

*2.8.2. (R)-tert-butyl-2-(N-(1-(benzo[d]thiazol-2-yl)-2-methylpropyl)-4-phenoxyphenylsulfonamido)acetate (**4o**)*

The pure compound obtained as a brown oil (86% yield). ^{1}H NMR ($CDCl_3$), δ (ppm): 7.93 (d, J = 9.0 Hz, 1H, BTA**H**), 7.88 (d, J = 9.0 Hz, 2H, PhOPh**H**), 7.83 (d, J = 9.0 Hz, 1H, BTA**H**), 7.44–7.38 (m, 4H, BTA**H**, PhOPh**H**), 7.20 (t, J = 7.5 Hz, 1H, PhOPh**H**), 6.98 (d, J = 9.0 Hz, 4H, PhOPh**H**), 4.72 (d, J = 9.0 Hz, 1H, BTAC**H**N), 4.36, 4.03 (dd, J = 18.0, 18.0 Hz, 2H, C**H**$_2$COO), 2.58–2.55 (m, 1H, C**H**$(CH_3)_2$), 1.02 (d, J = 6.0 Hz, 3H, C**H**$_3$), 0.84 (d, J = 6.0 Hz, 3H, C**H**$_3$); m/z (ESI MS): 575.3 $(M + Na)^+$.

2.9. Synthesis and characterization of the carboxylic acid analogs (3a–4a)

*2.9.1. 2-(N-(benzo[d]thiazol-2-ylmethyl)-4-phenoxyphenylsulfonamido) acetic acid (**3a**)*

A solution of **3o** (0.150 g, 0.29 mmol) in 40:60 trifluoroacetic acid (TFA)/CH_2Cl_2 (4 mL) was stirred at r.t. for 6 h. The solvent was evaporated, the residue was dissolved in EtOAc (15 mL) and washed with H_2O (4 × 20 mL). After drying the organic phase over anhydrous Na_2SO_4 and evaporating the solvent, the residue was recrystallized from Et_2O to afford the pure compound as a white solid (0.077 g, 58% yield), m.p. 178–180 °C. ^{1}H NMR ($CDCl_3$), δ (ppm): 7.95 (d, J = 8.0 Hz, 1H, BTA**H**), 7.90 (d, J = 9.0 Hz, 1H, BTA**H**), 7.83 (d, J =9.0 Hz, 2H, PhOPh**H**), 7.49–7.44 (m, 4H, BTA**H**, PhOPh**H**), 7.22 (t, J = 7.5 Hz, 1H, PhOPh**H**), 7.02 (d, J = 9.0 Hz, 4H, PhOPh**H**), 4.98 (s, 2H, BTAC**H**$_2$), 4.14 (s, 2H, C**H**$_2$COOH); m/z (ESI MS): 477.2 $(M + Na)^+$.

*2.9.2. (R)-2-(N-(1-(benzo[d]thiazol-2-yl)-2-methylpropyl)-4-phenoxyphenylsulfonamido)acetic acid (**4a**)*

The pure compound was obtained as light brown solid (92% yield), m.p. 146–147 °C; ^{1}H NMR ($CDCl_3$), δ (ppm): 7.92 (d, J = 9.0 Hz, 1H, BTA**H**), 7.86 (d, J = 6.0 Hz, 1H, BTA**H**), 7.49 (d, J = 9.0 Hz, 2H, PhOPh**H**), 7.49–7.43 (m, 4H, BTA**H**, PhOPh**H**), 7.21 (t, J = 7.5 Hz, 1H, PhOPh**H**), 6.95–6.91 (m, 4H, PhOPh**H**), 4.91 (d, J = 9.0 Hz, BTAC**H**N), 4.50, 4.15(dd, J = 18.0, 18.0 Hz, 2H, C**H**$_2$COO), 2.43–2.39 (m, 1H, C**H**$(CH_3)_2$), 1.04 (d, J = 6.0 Hz, 3H, C**H**$_3$), 0.98 (d, J = 6.0 Hz, 3H, C**H**$_3$); m/z (ESI MS): 497.2 $(M + H)^+$, 519.3 $(M + Na)^+$.

2.9.3. Tert-butyl carbazate (NH_2NHBoc)

A solution of di-*tert*-butyl dicarbonate (2.91 g, 13.3 mmol) in dioxane (50 mL) was dropwise added to a solution of K_2CO_3 (7.35 g, 53.2 mmol) and hydrazine hydrate (2.58 mL, 53.2 mmol) in water (50 mL), and the mixture was stirred at r.t. for 12 h. Two phases were formed, separated, and then the aqueous phase was washed with ethyl ether (2 × 25 mL). The ether phase was added to the dioxane phase, and the total organic solution was evaporated. The colorless oil obtained was distilled under vacuum, and the pure product was obtained as the sublimated white crystals (1.64 g, 93% yield), m.p. 38–39 °C. ^{1}H NMR (CDCl3) δ (ppm): 5.83 (bs, 1H, N**H**Boc), 3.67 (d, J = 3.0 Hz, 2H, N**H**2), 1.45 (s, 9H, t-Bu**H**); m/z (ESI MS): 155.0 $(M + Na)^+$.

2.10. Synthesis and characterization of compounds 3bp, 4bp, 3cp, 4cp, and 3d

The preparation of compounds **3bp**, **4bp**, **3cp**, and **4cp** followed method B described for compound **2bp**, using the respective carboxylic acids (**3a** and **4a**), the respective amines, and EDC.HCl. In case of **3bp** and **4bp** the amine was *O*-(2,4-dimethoxybenzyl)-hydroxylamine (NH_2ODmb), previously prepared according to literature [17], while *tert*-butyl carbazate (NH_2NHBoc) was used for **3cp** and **4cp**. In case of **3d**, the method A described for **2bp** was applied, with 4-methoxybenzenesulfonylhydrazide as amine, and T3P and Et_3N as reagents.

*2.10.1. 2-(N-(benzo[d]thiazol-2-ylmethyl)-4-phenoxyphenylsulfonamido)-N-(2,4-dimethoxy benzyloxy)acetamide (**3bp**)*

Pure compound obtained as yellow oil (80% yield). ^{1}H NMR ($CDCl_3$), δ (ppm): 7.84 (d, J = 7.5 Hz, 1H, BTA**H**), 7.79–7.73 (m, 3H, BTA**H**, PhOPh**H**), 7.52–7.36 (m, 4H, BTA**H**, PhOPh**H**), 7.22 (t, J = 7.5 Hz, 1H, PhOPh**H**), 7.01 (d, J = 6 Hz, 2H, PhOPh**H**), 6.96–6.89 (m, 3H, PhOPh**H**, Dmb**H**CH_2), 6.46–6.35 (m, 2H, Dmb**H**CH_2), 4.91 (s, 2H, BTAC**H**$_2$), 4.73 (s, 2H, DmbC**H**$_2$), 4.01 (s, 2H, C**H**$_2$CONH), 3.78 (s, 3H, OC**H**$_3$), 3.73 (s, 3H, OC**H**$_3$); m/z (ESI MS): 642.4 $(M + Na)^+$, 658.3 $(M + K)^+$.

*2.10.2. (R)-2-(N-(1-(benzo[d]thiazol-2-yl)-2-methylpropyl)-4-phenoxyphenylsulfonamido)-N-(2,4-dimethoxybenzyloxy)acetamide (**4 bp**)*

Pure compound obtained as yellow oil (42% yield). ^{1}H NMR ($CDCl_3$), δ (ppm): 8.01 (d, J = 9.0 Hz, 1H, BTA**H**), 7.90 (d, J = 8.5 Hz, 1H, BTA**H**), 7.55 (d, J = 9.0 Hz, 2H, PhOPh**H**), 7.50–7.45 (m, 4H, BTA**H**, PhOPh**H**), 7.20 (t, J = 7.5 Hz, 1H, PhOPh**H**), 7.07–6.90 (m, 5H, PhOPh**H**, Dmb**H**CH_2), 6.46–6.41 (m, 2H, Dmb**H**CH_2), 5.04 (s, 2H, DmbC**H**$_2$), 4.99 (d, J = 9.0 Hz, BTAC**H**N), 4.55, 4.18 (dd, J = 17.8, 18.0 Hz, 2H, C**H**$_2$CONH), 3.81 (s, 3H, OC**H**$_3$), 3.79 (s, 3H, OC**H**$_3$), 2.38–2.30 (m, 1H, C**H**$(CH_3)_2$), 1.05 (d, J = 6.0 Hz, 3H, C**H**$_3$), 0.99 (d, J = 6.0 Hz, 3H, C**H**$_3$); m/z (ESI MS): 684.4 $(M + Na)^+$.

*2.10.3. Tert-butyl-2-(2-(N-(benzo[d]thiazol-2-ylmethyl)-4-phenoxyphenylsulfonamido)-acetyl)hydrazinecarboxylate (**3cp**)*

Pure compound obtained as yellow oil (82% yield). ^{1}H NMR ($CDCl_3$), δ (ppm): 7.91 (d, J = 6.0 Hz, 1H, BTA**H**), 7.86 (d, J = 6.0 Hz, 1H, BTA**H**), 7.78 (d, J = 6.0 Hz, 2H, PhOPh**H**), 7.46–7.40 (m, 4H, BTA**H**, PhOPh**H**), 7.20 (t, J = 7.5 Hz, 1H, PhOPh**H**), 7.02–6.95 (m, 4H, PhOPh**H**), 4.89 (s, 2H, BTAC**H**$_2$), 4.13 (s, 2H, C**H**$_2$CONH), 1.47 (s, 9H, *t*Bu**H**); m/z (FAB): 591.3 $(M + Na)^+$.

*2.10.4. (R)-tert-butyl-2-(2-(N-(1-(benzo[d]thiazol-2-yl)-2-methylpropyl)-4-phenoxyphenyl-sulfonamido)acetyl)hydrazinecarboxylate (**4cp**)*

Pure compound obtained as yellow oil (33% yield). ^{1}H NMR ($CDCl_3$), δ (ppm): 7.93 (d, J = 6.0 Hz, 1H, BTA**H**), 7.85 (d, J = 6 Hz, 1H, BTA**H**), 7.69 (d, J = 9.0 Hz, 2H, PhOPh**H**), 7.46–7.41 (m, 4H, BTA**H**, PhOPh**H**), 7.21 (t, J = 7.0 Hz, 1H, PhOPh**H**), 6.91–6.86 (m, 4H, PhOPh**H**), 4.89 (d, J = 9.0 Hz, 1H, BTAC**H**N), 4.42, 4.02 (dd, J = 18.0, 18.0 Hz, 2H, NC**H**$_2$CONH), 2.35–2.28 (m, 1H, C**H**$(CH_3)_2$), 1.48 (s, 9H, *t*Bu**H**), 1.01 (d, J = 6.0 Hz, 3H, C**H**$_3$), 0.88 (d, J = 6.0 Hz, 3H, C**H**$_3$); m/z (ESI MS): 611.3 $(M + H)^+$, 633.3 $(M + Na)^+$.

*2.10.5. N-(2-(2-(4-methoxyphenylsulfonyl)hydrazinyl)-2-oxoethyl)-4-phenoxybenzenesulfonamide (**3d**)*

Flash chromatography (9:0.1 CH_2Cl_2/MeOH as eluent, R_f = 0.25) gave the pure compound as a beige solid (55% yield), m.p. 82–83 °C. ^{1}H NMR ($CDCl_3$), δ (ppm): 11.59 (d, J = 4.0 Hz, 1H, CON**H**NHSO$_2$), 7.87 (d, J = 8.0 Hz, 1H, BTA**H**), 7.83 (d, J = 8.4 Hz, 2H, Ph**H**), 7.76 (d, J = 8.4 Hz, 2H, PhOPh**H**), 7.57 (t, J = 7.6 Hz, 1H, BTA**H**), 7.46 (t, J = 7.6 Hz, 1H, BTA**H**), 7.40 (t, J = 7.6 Hz, 2H, PhOPh**H**), 7.23 (t, J = 7.2 Hz, 1H, PhOPh**H**), 7.18 (d, J = 5.6 Hz, 1H, CONHN**H**SO$_2$), 6.99–6.96 (m, 4H, PhOPh**H**), 6.92 (d, J = 8.4 Hz, 2H, Ph**H**), 4.73 (s, 2H, BTAC**H**$_2$), 3.93 (s, 2H, C**H**$_2$CONH), 3.83 (s, 3H, OC**H**$_3$); m/z (ESI MS): 638.4 $(M + H)^+$, 660.6 $(M + Na)^+$.

2.11. Synthesis and characterization of the hydroxamic acids (3b, 4b)

*2.11.1. 2-(N-(benzo[d]thiazol-2-ylmethyl)-4-phenoxyphenylsulfonamido)-N-hydroxyacetamide (**3b**)*

The general procedure for removal of the Dmb group was followed. A solution of **3bp** (0.017 g, 0.027 mmol) in a 5:95 TFA/CH_2Cl_2 mixture (1 mL) was stirred at r.t. for 2 h. The resulting magenta solution was evaporated and MeOH was added to the residue. The mixture was filtered to remove the white polymer formed, and the solvent was evaporated, resulting in a yellowish oil. The pure product was obtained from recrystallization with Et_2O and n-hexane as beige solid (0.012 g, 99% yield), m.p. 126–128 °C. ^{1}H NMR ($CDCl_3$), δ (ppm): 7.97 (d, J = 9.0 Hz, 1H, BTA**H**), 7.89 (d, J = 9.0 Hz, 1H, BTA**H**), 7.74 (d, J = 9.0 Hz, 2H, PhOPh**H**), 7.49–7.44 (m, 4H, BTA**H**, PhOPh**H**), 7.23 (d, J = 9.0 Hz, 1H, PhOPh**H**), 7.00–6.93 (m, 4H, PhOPh**H**), 5.30 (s, 2H, BTAC**H**$_2$), 4.82 (s, 2H, C**H**$_2$CONH); m/z (ESI MS): 470.2 $(M + H)^+$, 492.2 $(M + Na)^+$.

*2.11.2. (R)-2-(N-(1-(benzo[d]thiazol-2-yl)-2-methylpropyl)-4-phenoxyphenylsulfonamido)-N-hydroxyacetamide (**4b**)*

Pure compound obtained as a beige solid (60% yield), m.p. 85–86 °C. ^{1}H NMR ($CDCl_3$), δ (ppm): 7.97 (d, J = 9.0 Hz, 1H, BTA**H**), 7.80 (d, J = 9.0 Hz, 1H, BA**H**), 7.55 (d, J = 9.0 Hz, 2H, PhOPh**H**), 7.50–7.44 (m, 4H, BTA**H**, PhOPh**H**), 7.20 (t, J = 7.0 Hz, 1H, PhOPh**H**), 6.92–6.81 (m, 4H, PhOPh**H**), 4.84 (d, J = 9 Hz, BTAC**H**N), 4.47, 4.13 (dd, J = 18.0, 17.5 Hz, 2H, C**H**$_2$CONH), 2.30–2.22 (m, 1H, C**H**$(CH_3)_2$), 1.00 (d, J = 6.0 Hz, 3H, C**H**$_3$), 0.88 (d, J = 6.0 Hz, 3H, C**H**$_3$); m/z (ESI MS): 534.2 $(M + Na)^+$.

2.12. Synthesis and characterization of the hydrazides (3c, 4c)

The same procedure used for deprotection of the *tert*-butyl esters and generation of the carboxylic acid derivatives **3a** and **4a** was applied here to remove the *Boc* groups from compounds **3cp** and **4cp**.

*2.12.1. N-(benzo[d]thiazol-2-ylmethyl)-N-(2-hydrazinyl-2-oxoethyl)-4-phenoxybenzenesulfonamide (**3c**)*

Pure compound as very hygroscopic light brown solid (98% yield). ^{1}H NMR ($CDCl_3$), δ (ppm): 7.97 (d, J = 9.0 Hz, 1H, BTA**H**), 7.88 (d, J = 9.0 Hz, 1H, BTA**H**), 7.79 (d, J = 9.0 Hz, 2H, PhOPh**H**), 7.49–7.43 (m, 4H, BTA**H**, PhOPh**H**), 7.22 (s, 1H, PhOPh**H**), 7.02 (t, J = 7.5 Hz, 4H, PhOPh**H**), 4.81 (s, 2H, BTAC**H**$_2$), 4.02 (s, 2H, C**H**$_2$CONH); m/z (ESI MS): 469.2 $(M + H)^+$, 491.2 $(M + Na)^+$.

*2.12.2. (R)-N-(1-(benzo[d]thiazol-2-yl)-2-methylpropyl)-N-(2-hydrazinyl-2-oxoethyl)-4-phenoxybenzenesulfonamide (**4c**)*

Pure compound obtained as a slightly hygroscopic beige solid (67% yield), m.p. 72–75 °C. ^{1}H NMR ($CDCl_3$), δ (ppm): 7.90 (d, J = 6.2 Hz, 1H, BTA**H**), 7.84 (d, J = 6.0 Hz, 1H, BTA**H**), 7.70 (d, J = 9.0 Hz, 2H, PhOPh**H**), 7.43–7.36 (m, 4H, Ar**H**, PhOPh**H**), 7.20 (t, J = 7.0 Hz, 1H, PhOPh**H**), 6.88–6.83 (m, 4H, PhOPh**H**), 4.85 (d, J = 9.0 Hz, 1H, BTAC**H**N), 4.38, 4.00 (dd, J = 18.0, 18.0 Hz, 2H, C**H**$_2$CONH), 2.30–2.23 (m, 1H, C**H**$(CH_3)_2$), 0.98 (d, J = 6.0 Hz, 3H, C**H**$_3$), 0.86 (d, J = 6.0 Hz, 3H, C**H**$_3$); m/z (ESI MS): 533.3 $(M + Na)^+$.

2.13. Solution equilibrium studies

2.13.1. Potentiometric studies

2.13.1.1. General information. The aqueous zinc stock solution (0.0156 M) was prepared from 1000 ppm zinc standard solution (Titrisol) and its concentration was standardized by titration with K_2H_2EDTA. The titrant (0.1 M KOH) was prepared from carbonate free commercial concentrate (Titrisol ampoule) in a 40% w/w DMSO/H_2O medium, standardized by potentiometric titration with potassium hydrogen phthalate in the same medium and discarded when the percentage of carbonate (Gran's method [18]) was higher than 0.5% of the total amount of base.

2.13.1.2. Potentiometric measurements. Potentiometric titrations of compounds **2b–2d** were accomplished in 40% w/w DMSO/H_2O solution at ionic strength (I) 0.1 M KCl, while keeping the working temperature at 25.0 ± 0.1 °C. The measurements were performed with 0.025 mmol of ligand in a final volume of 40.00 mL, firstly in the absence of the metal ion and afterwards in its presence, with corresponding C_M:C_L molar ratios of 0:1, 1:1 and 1:2. All titrations were performed in triplicate and under the stated experimental conditions

the pK_w value (14.3) was determined and subsequently used in the computations.

2.13.1.3. Calculation of equilibrium constants. The stepwise protonation constants of the ligands, $K_i = [H_iL] / [H_{i-1}\,L][H]$, and the overall zinc-complex stability constants, $\beta_{Zn_mH_hL_l} = [Zn_mH_hL_l] / [Zn]^m[H]^h[L]^l$, were calculated by fitting the potentiometric data obtained in the absence and in the presence of Zn(II), using the HYPERQUAD 2008 program [19]. The Zn(II) hydrolytic species were determined under the defined experimental conditions ($I = 0.1$ M KCl, 40% w/w DMSO/H_2O, $T = 25.0 \pm 0.1$ °C, log $\beta_{ZnH-2} = -14.48$, log $\beta_{ZnH-3} = -21.75$) and were included in the equilibrium model. Species distribution curves were plotted with the Hyss program [19].

2.13.2. Spectroscopic studies

A ^{1}H NMR titration of a solution of **2c** (12 mM) in 40% DMSO-d6/D_2O was performed. The pD* value (reading of the pH meter previously calibrated with aqueous buffers pH 4 and 7) was changed by addition of DCl or KOD solutions. This assay was repeated twice and reproducibility was verified. The evaluation of the stability of compounds **2b** and **2c** ($C_L = 10$–15 mM) in 40% DMSO-d6/D_2O medium was also performed through analysis of its ^{1}H NMR spectra ($1 < pD < 9$) along time at r.t. Spectra of **2c** (12 mM) and of the system Zn(II)-**2c** (1:1 and 5:1) were taken in 100% DMSO-d6.

2.14. MMPs inhibition

The adopted method for assessing the MMP inhibitory capacity was according to reported in literature [20]. Recombinant human MMP14 catalytic domain (MMP14cd) was a kind gift of Prof. Gillian Murphy (Department of Oncology, University of Cambridge, UK). Recombinant human pro-MMP-2 was purchased from Calbiochem.

Pro-MMP2 was activated immediately prior to use with *p*-aminophenylmercuric acetate (APMA 2 mM for 1 h at 37 °C). For the assay measurements, the inhibitor stock solutions (10 mM in DMSO) were further diluted, at seven different concentrations for each MMP in the fluorometric assay buffer (FAB: Tris 50 mM, pH = 7.5, NaCl 150 mM, $CaCl_2$ 10 mM, Brij 35 0.05% and DMSO 1%). Activated enzyme (final concentration 0.5 nM for MMP2, 1.0 nM for MMP-14cd) and inhibitor solutions were incubated in the assay buffer for 2 h at 25 °C. After the addition of the fluorogenic substrate Mca–Lys–Pro–Leu–Gly–Leu–Dap(Dnp)–Ala–Arg–NH_2 (Bachem) for all enzymes in DMSO (final concentration 2 μM), the hydrolysis was monitored every 15 s, for 15 min, recording the increase in fluorescence ($\lambda_{ex} = 325$ nM, $\lambda_{em} = 395$ nM) with a Molecular Devices SpectraMax Gemini XS plate reader. The assays were performed in triplicate in a total volume of 200 μL per well in 96-well microtiter plates (Corning black, NBS). The MMP inhibition activity was expressed in relative fluorescent units (RFU). Percent of inhibition was calculated from control reactions without the inhibitor. IC_{50} was determined using the formula: $v_i/v_o = 1 / (1 + [I] / IC_{50})$, where v_i is the initial velocity of substrate cleavage in the presence of the inhibitor at concentration [I] and v_o is the initial velocity in the absence of the inhibitor. Results were analyzed using SoftMax Pro software [21] and GraFit software [22].

2.15. Molecular simulation

The ligands were built using Maestro 7.5 [23] and were minimized by the use of Macromodel [24], with the conjugated gradient method until a convergence value of 0.05 kcal/Å mol was reached, with a water environment model (generalized-Born/surface-area model), applying the MMFFs force field (MMFFs is a variant of the all-atom model Merck Molecular Force Field that enforces planarity about delocalized sp_2 nitrogens) and a distance-dependent dielectric constant of 1.0. They were then submitted to a conformational search (CS) of 100 steps, using an algorithm based on the Monte Carlo method, with the same force field and parameters used for the minimization. To our knowledge, to date no single crystal of MMP2 complex with a small ligand has been obtained and diffracted. Hence, the receptor structure used in these calculations was the gelatinase-A (MMP2) catalytic domain, which was extracted from the RCSB Protein Data Bank (PDB) [25] (entry 1QIB), and it was treated using Maestro 7.5. The solvent molecules and counterions were removed from the original structure, as well as the structural Ca^{2+} ions in the protein, and hydrogen atoms were added. Since this MMP2 structure did not possess any ligand, it was aligned with the MMP9 complex, using Chimera software [26] (PDB structure 1GKC), and the ligand in this structure was further used to define the zone of interest in MMP2 for the docking calculations, as the residues within 15 Å from the position of this ligand. The minimized ligands were docked into MMP2 with GOLD program, version 4.0 [27] following a procedure previously reported [9]. The "allow early termination" option was deactivated while the possibility for the ligand to flip ring corners was activated. The remaining default parameters were used, and the ligands were submitted to 100 genetic algorithm runs applying the ASP fitness function, together with a Scaffold Match Constraint (SMC). This constraint was used in order to set the position of the HA or carboxylic acid ZBGs, and the hydroxamate (CONO atoms) and carboxylate (the CCOO atoms) scaffolds were defined. These scaffolds were taken, respectively, from the PDB structures 1JIZ and 1BZS, after they were aligned with the MMP2 structure with Chimera program. These crystal structures were chosen because of the similarity of the main structure of their ligands with our compounds. The *SMC Weight*, a parameter defining how closely the ligand atoms should fit onto the scaffold, was set to 10.0. The docking of the hydrazides and the other analogs was also performed, but not by the SMC method, and therefore with no guarantee of their accuracy, since no crystal structures of MMPs complexed with inhibitors bearing these ZBGs are available.

2.16. Cellular viability assays

A2780 Human ovarian carcinoma cells (Sigma-Aldrich) were maintained in RPMI 1640 cell culture medium supplemented with 10% fetal bovine serum (FBS) and 1% antibiotics (Invitrogen). The cells were kept in a CO_2 incubator (Heraus, Germany) at 37 °C/5% CO_2 in a humidified atmosphere. For the cellular viability studies, cells from a confluent monolayer were removed from flasks by a trypsin–EDTA solution, suspended in 200 μL of complete medium and seeded in 96-well plates. The plates were incubated at 37 °C for 24 h prior to compound testing to allow cells to adhere. A stock solution in DMSO (20 mM) of each compound was freshly prepared and used for sequential dilutions in medium. The final concentration of DMSO in cell culture medium did not exceed 1%. Control groups with and without DMSO (1%) were included in the assays as negative controls. The cytotoxic activity of the compounds was screened within the concentration range 0.2–200 μM using the 3-(4,5-dimethylthiazol-2-yl)-2,5-diphenyltetrazolium bromide (MTT) assay [28].

Analysis of cell survival was carried out after a 72 h cell exposure to the compounds by the MTT assay, which is based on the reduction of MTT by viable cells to form formazan crystals. Briefly, a solution of MTT dissolved in PBS (0.5 mg/mL) was added to each well (200 μL) and the plates were incubated at 37 °C for 3–4 h. Then the solution was discarded and 200 μL of DMSO was added to each well to dissolve the formazan crystals. The absorbance was measured at 570 nm with a plate spectrophotometer (Power Wave Xs, Bio-TeK). Each experiment was repeated twice and each concentration was tested in at least six replicates. Results are expressed as a percentage of cell survival relative to control cells in the absence of the compound. IC_{50} values (half-inhibitory concentration, i.e. drug concentration that induces 50% of cell death) were calculated from dose–response curves constructed by plotting cell survival (%) versus compound concentration (M). The IC_{50} values were calculated with the *GraphPad Prism* software.

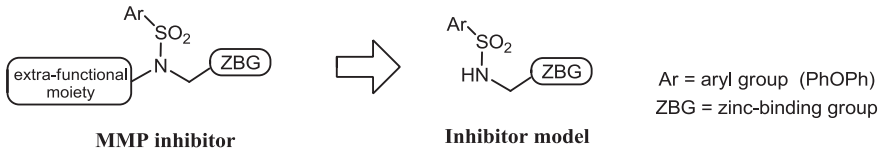

Chart 1. Truncation strategy for the MMPI models design.

3. Results and discussion

3.1. Molecular design

With the aim of developing new MMPIs with improved biological properties, namely as anti-cancer, our first design strategy was to work out on model compounds, containing different zinc-binding groups (ZBG), for the sake of replacing the usual hydroxamate (HA) group by other chelating groups, also with good ability to bind the catalytic zinc of the MMPs, but with better pharmacokinetic profiles. In order to get further biological improvements, a group of those MMPI models should be selected to append an extra bio-relevant group, namely with anti-cancer properties.

Therefore, we first selected a set of inhibitor models bearing different ZBGs and assessed their solution Zn-binding capacity and MMP inhibitory capacity. The option for the main skeleton was based on our previous disclosures on potent HA-based MMP inhibitors, but with truncations on some molecular segments. The arylsulfonyl moiety was kept, because of its recognized important role in the ligand binding to the S1′ cavity of the MMPs, in particular the 4-phenoxyphenyl (PhOPh) was selected as the aryl group (see Chart 1) [9,17].

The ZBG selection took into account that those groups should share some structural features of the HA group, in order to provide as many favorable interactions with the enzymes as possible [29]. Given the similarities between the hydrazide and the hydroxamate groups, several hydrazide derivatives have been studied. The carboxylic acid (**2a**) and the HA (**2b**) derivatives (see Fig. 2) were also selected for comparison. Among the hydrazide derivatives we included a simple primary hydrazide (**2c**) and two secondary hydrazides, namely an arylsulfonylhydrazide (**2d**) and its isosteric analog arylhydrazide (**2f**). These groups have only been scarcely investigated for MMP inhibition and for their zinc complexation ability [30,31]. Moreover, because the terminal NH_2 group of the hydrazide is less electrophilic than the OH group in hydroxamate, the hydrazide derivatives are expected to be more resistant to hydrolysis than the hydroxamate analogues. Finally, as hydrazide-related ZBGs, we have also explored two acylhydrazone derivatives (**2e** and **2g**). In fact, the acylhydrazones are well known to bind metal ions with great efficiency, including the zinc(II) [32,33], and some anticancer properties of hydrazone derivatives have been reported [34]. A representative selection of these model compounds are herein studied in terms of their ability to bind Zn(II) ion in solution, in order to disclose their relative chelating ability, and to compare with that of HA.

Aimed at a final accomplishment of our outlined major goals we pursued with the second design strategy, by developing a set of multifunctional compounds, which conjugate, in the same molecular entity, characteristics of MMP inhibitors and antitumor agents that could end up with anticancer activity enhancements, by taking advantage of addition or synergistic effects. Hence, in order to provide that second biological role we decided to attach a benzothiazole group (BTA) to our scaffold, and compounds **3**–**4** (Fig. 2) were designed. In fact, BTA derivatives have attracted strong interest due to their biological and pharmacological properties, namely as antimicrobials, anti-inflammatory and antitumor agents [13–15]. In order to tune the effect of the structural and lipophilic modifications nearby the BTA moiety over the MMP inhibitory activity, we decided to make a further variation on the linker connecting the BTA moiety to the main scaffold of the inhibitor (X-R1, see Fig. 2), by substituting the simple methylene (compounds **3**) by a CH-isopropyl group (compounds **4**). Only some of the most promising ZBGs from series **2** were included in series **3** and **4**.

3.2. Synthesis

The preparation of all compounds herein presented started from an amino acid or its ester derivative. In the case of compounds **2** (see Scheme 1) the glycine ethyl ester was used as starting material, which was coupled with the arylsulfonyl chloride to give the secondary

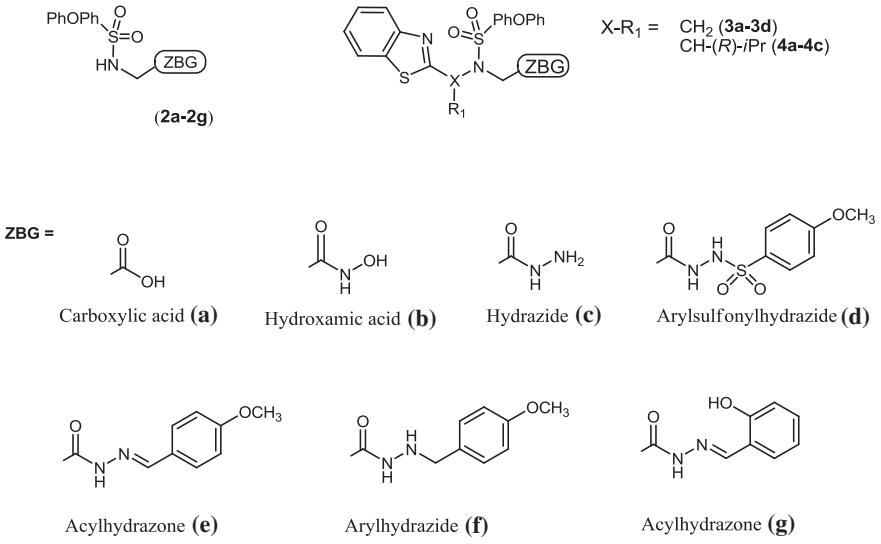

Fig. 2. Structures of the compounds studied in this work: the model compounds (**2**), and the benzothiazole (BTA)-based inhibitors (**3–4**); the series entries are defined by the ZBG (**a–g**).

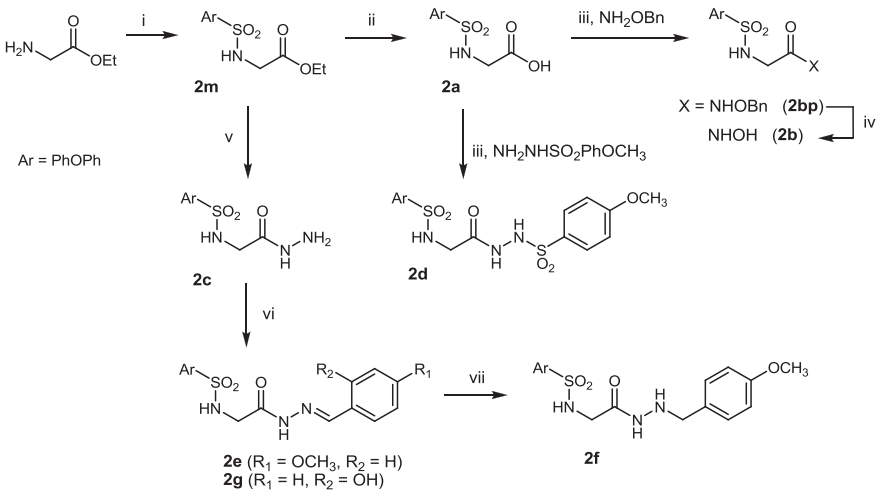

Scheme 1. Synthesis of compounds **2a**–**2d**. Reagents and conditions: i) $PhOPhSO_2Cl$, Et_3N, CH_3CN, r.t.; ii) KOH, MeOH, r.t.; iii) T3P, Et_3N, CH_2Cl_2, r.t.; iv) H_2, Pd/C, MeOH, r.t.; v) NH_2NH_2, EtOH, r.t.; vi) anisaldehyde (**e**) or salicylaldehyde (**g**), EtOH, 50 °C; and vii) $NaBH_4$, AcOH, r.t.

arylsulfonamide **2m** (in this case aryl = 4-phenoxybenzene group). This compound was hydrolyzed with a KOH methanolic solution to generate the carboxylic acid **2a**, which was coupled with *O*-benzylhydroxylamine or the 4-methoxybenzenesulfonylhydrazide to afford, respectively, the benzyl *O*-protected hydroxamic acid (**2bp**) or the arylsulfonylhydrazide (**2d**). Regarding the carboxyl-amine coupling reactions, two different methodologies were used for carboxyl activation. For compound **2bp**, method A, propylphosphonic anhydride (T3P®) was used as activating agent, with triethylamine (Et_3N), and, after stirring at room temperature for 2 h, the reaction was complete. A straightforward workup was followed and the final compound was obtained with good yield (76%). Method B made use of 1-ethyl-3-(3-dimethylaminopropyl)carbodiimide hydrochloride (EDC.HCl) with a catalytic amount of 4-dimethylaminopyridine (DMAP), and the reaction typically took 8 to 16 h to be over. After a quite simple workup a 67% yield was obtained. Since the synthesis of **2d** did not work well with method B, method A was followed for all the sulfonylhydrazides. The hydroxamic acid **2b** was obtained after the benzyl removal from **2 bp** by catalytic hydrogenation with 1.5 bar H_2 and 5% palladium over charcoal (Pd/C). Regarding the hydrazide **2c**, it was easily formed from reaction of the ethyl ester **2m** with hydrazine hydrate. The hydrazones **2e** and **2g** were obtained from reaction of the hydrazide **2c** with the aromatic 4-anisaldehyde and salicylaldehyde, respectively. The dominant isomers formed were, in both cases, the *E* isomers (which could be observed by NMR), almost exclusively for **2e**, and >90% for **2g**. Concerning the arylhydrazide **2f**, its preparation from **2e**, through a standard procedure for reduction of Schiff bases, using $NaBH_4$ or BH_3CN in THF, DMF or EtOH, did not work well, disregarding a number of modifications in solvent type, temperature or reaction time, nor did the hydrogenation using H_2 with Pd/C. This may be attributed to the extra stability of the hydrazone when linked to a carbonyl group. However, **2f** was successfully obtained by addition of excess $NaBH_4$ in acetic acid, as reported in literature [35].

The synthetic procedure for the BTA-containing inhibitors (**3–4**) is depicted in Scheme 2. It started with the preparation of the benzothiazole-amine fragments (**3m–4m**) from the corresponding

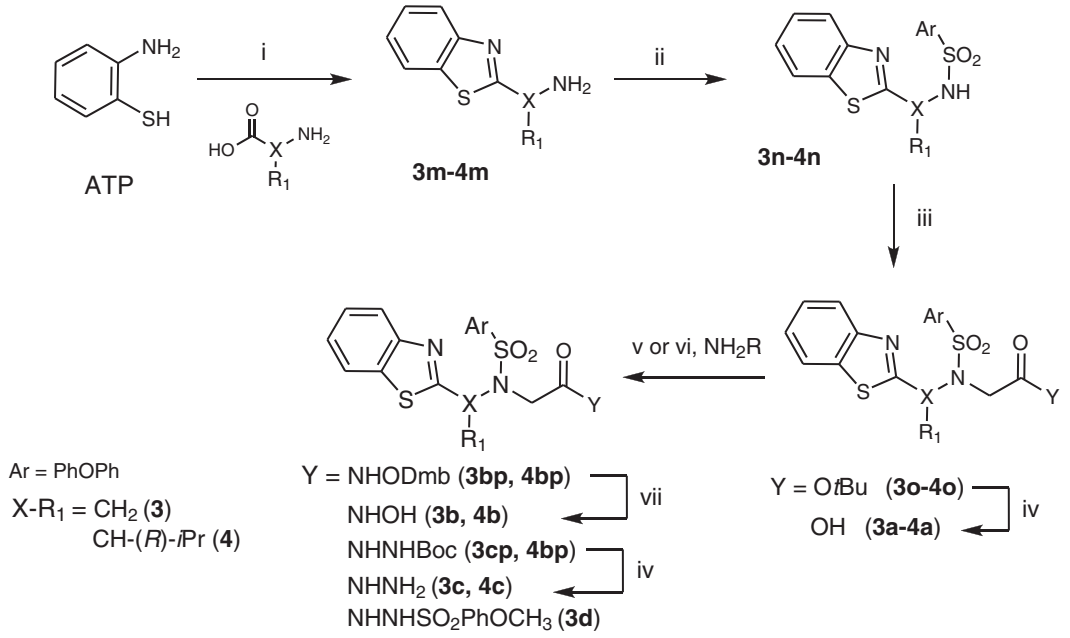

Scheme 2. Synthesis of compounds **3**–**4**. Reagents and conditions: i) polyphosphoric acid, 220 °C; ii) $PhOPhSO_2Cl$, Et_3N, CH_3CN, r.t.; iii) $BrCH_2COOtBu$, K_2CO_3, KI cat, DMF, r.t.; iv) 40% TFA, CH_2Cl_2, r.t.; v) EDC.HCl, DMAP cat, CH_2Cl_2, r.t.; vi) T3P, Et_3N, CH_2Cl_2, r.t.; and vii) 5% TFA, CH_2Cl_2, r.t. Dmb = 2,4-dimethoxybenzyl group; NH_2R = NH_2ODmb (**b**), NH_2NHBoc (**c**), and $NH_2NHSO_2PhOCH_3$ (**d**).

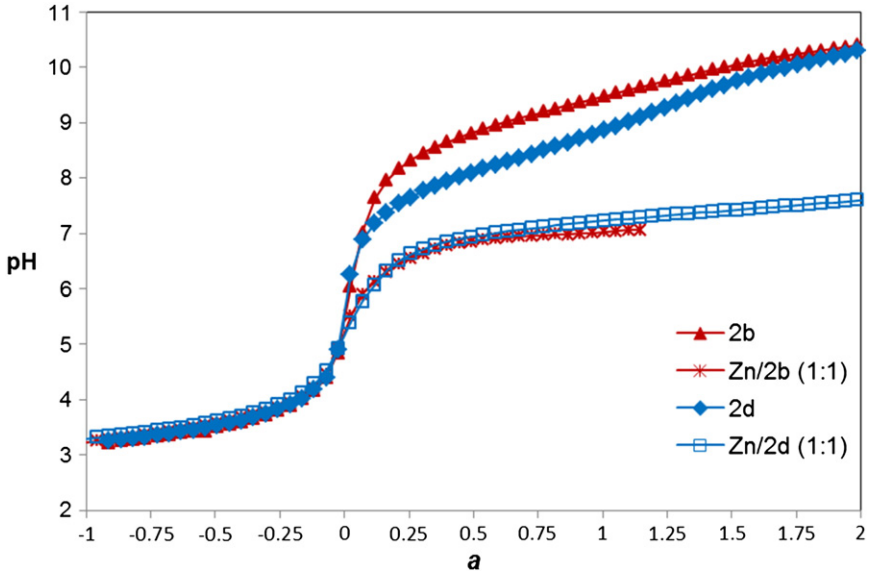

Fig. 3. Potentiometric titration curves for ligands **2b** and **2d** and their Zn(II) complexes ($C_L/C_{Zn} = 1$, $C_L = 6.25 \times 10^{-4}$ M, in 40% DMSO/H_2O).

amino acid (or ester) and 2-aminothiophenol (ATP), making use of a dehydrating agent, the polyphosphoric acid. Glycine ethyl ester and D-valine were used to obtain the compound series **3** and **4**, respectively. The arylsulfonamide analogues (**3n–4n**) were prepared, similarly to **2m**, from the coupling reaction of the BTA-amines with the respective arylsulfonyl chloride. These sulfonamides were then reacted with *tert*-butyl bromoacetate in anhydrous DMF, using the inorganic base K_2CO_3 to yield compounds **3o–4o**; their *tert*-butyl deprotection with 50% TFA in CH_2Cl_2 afforded the corresponding carboxylic analogues **3a–4a**. These compounds were submitted to coupling reactions with different amine-bearing derivatives, using either method A (with T3P® [36]) or B (with EDC.HCl), as discussed for compound **2bp**. These reactions provided the respective hydroxamic acids *O*-protected with 2,4-dimethoxybenzyl group (Dmb) (**3bp** and **4bp**), the hydrazides protected with *tert*-butyloxycarbonyl group (Boc) (**3bp** and **4bp**), or the arylsulfonylhydrazide **3d**. Removal of those protecting groups gave rise to the final hydroxamic acids (**3b** and **4b**) or hydrazides (**3c** and **4c**), using 5% TFA/CH_2Cl_2 or 40% TFA/CH_2Cl_2, respectively.

3.3. Solution equilibrium studies

In order to analyze the effect of the different herein proposed ZBGs on the chelating efficacy towards the Zn(II), some model compounds were chosen, namely **2b** (hydroxamic acid), **2c** (hydrazide) and **2d** (arylsulfonylhydrazide). Prior to the study of the Zn(II) complexation, the ligand acid–base behavior was studied, mainly by potentiometry. Since the water solubility of the three compounds was relatively low (**2c** > **2b** > **2d**), all the studies were performed in 40% (w/w) DMSO/H_2O mixed solvent.

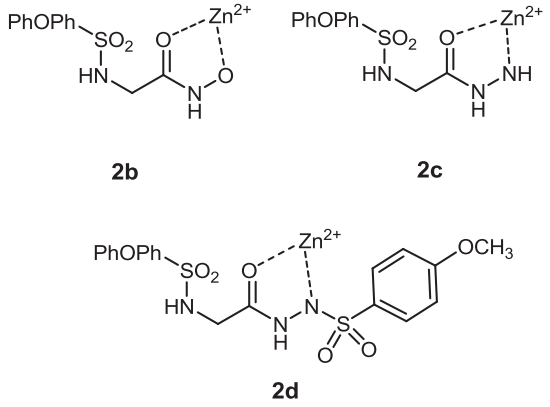

Fig. 4. Proposed structures for ZnHL complexes of a) **2b**, b) **2c** and c) **2d.**

3.3.1. Acid–base properties

The stepwise protonation constants of compounds **2b**, **2c** and **2d** were obtained by fitting analysis of the potentiometric data with the Hyperquad 2008 program [19] and the values are shown in Table 1. The protonation process of these compounds was mainly studied by potentiometry, but a ^{1}H NMR spectroscopic titration was also performed in order to ascertain the protonation sequence of **2c.**

All the ligands were obtained as neutral species, although the fully protonated form is H_2L for **2b** and **2d**, and H_3L^+ for **2c**. The $PhOPhSO_2NH$ moiety is a common structural feature of compounds **2b–2d** and analysis of Table 1 shows that the log K_1 values herein determined are fairly similar for the three compounds (9.7–10.4), thus suggesting they should be attributed to the protonation of $PhOPhSO_2N^-$. In fact, these values are in the same order of magnitude of others previously found for primary sulfonamides (9.64–10.16) [37], but higher than the value obtained for the secondary biphenyl sulfonamide (9.10) [38], due to the electron acceptor character of the phenyl group adjacent to the nitrogen atom.

The second constant (log K_2) is attributed to protonation of different groups, namely the hydroxamate hydroxy group, for **2b**, and the $MeOPhSO_2N^-NH$ group for **2d.** The log K_2 value (8.91) herein calculated for **2b** is similar to the reported values in aqueous solution for other hydroxamate groups (iminocarboxymethyl hydroxamic acid (ICMHA, 9.09) [39], glycine-hydroxamic acid (GLYHA, 9.26) [40] and other hydroxamate enzyme inhibitors (8.47–9.11) [37]). Regarding **2d**, the calculated log K_2 value (8.12) is in agreement with that predicted for the sulfonyl derivative of acylhydrazine ($RCONHNHSO_2R'$, 7.93). A slightly higher value was found for acylhydrazine ($RCONHNHCOR'$, 9.80), the difference being attributed to the high electronegativity of the sulfonyl group [41]. Therefore, in **2d** the second protonation occurs in $RCONHN^-SO_2R'$, whereas the log K value corresponding to the protonation of the other hydrazinic group is quite high [42] and could not be determined by potentiometry.

Concerning compound **2c**, its protonation was studied by ^{1}H NMR titration in 40% DMSO/D_2O medium. In spite of the limitations associated to this method, the experiment was reproducible and the titration curve profiles indicated that **2c** has two pH ranges where

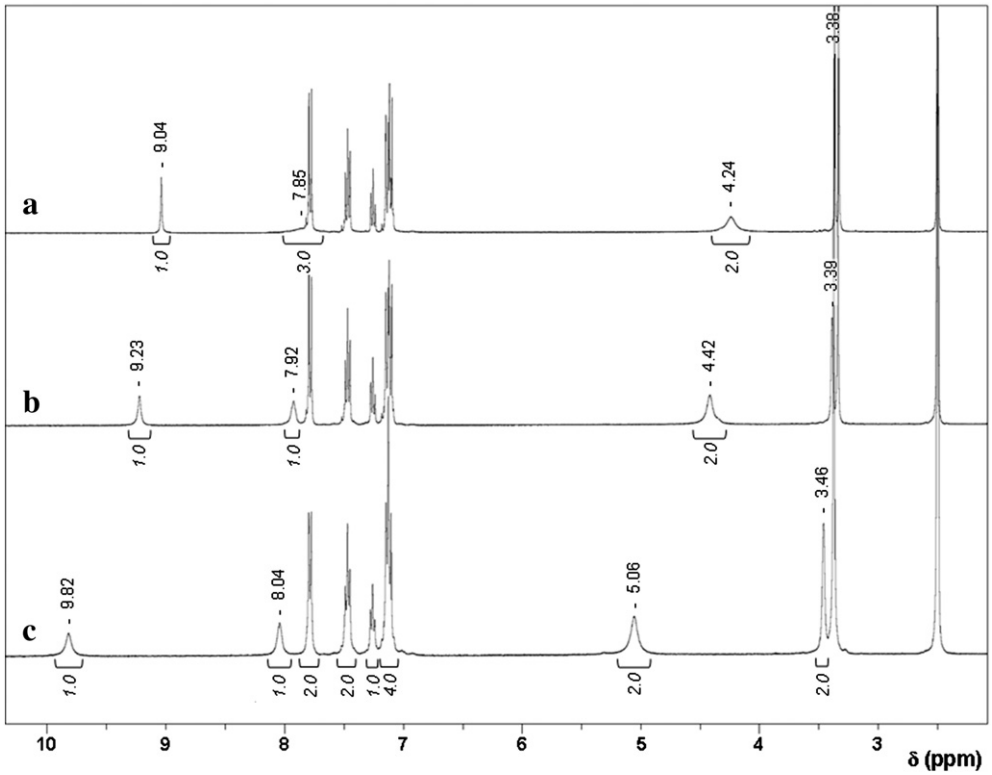

Fig. 5. ^{1}H NMR spectra of a) **2c**, b) Zn(II)-**2c** (1:1) and c) Zn(II)-**2c** (5:1) in DMSO-d6. The most important peak integrals are displayed (italic) under each spectrum.

protonation takes place (Fig. S1): at the high pD* range (10–12), protonation must occur at both N^- groups (hydrazide CON^- and sulfonamide SO_2N^-), according to the inflexion of the titration curves showed by all the nonlabile protons 1–4 (phenylic 2–4 and methylenic 1). At the lower pD* range (2–4), however, only a downfield shift of the methylenic protons 1 (SO_2NHCH_2CO) is observed, which gives support to the protonation of the NH_2 hydrazinic group. Thus, the protonation of compound **2c** seems to occur sequentially on the following groups: sulfonamide (SO_2N^-, $\log K_1 = 10.37$), hydrazide (CON^-, $\log K_2 = 8.00$) and hydrazinic NH_2 ($\log K_3 = 2.83$). Such a log *K* attribution is in agreement with that reported for benzoylhydrazine ($\log K_1 = 12.53$ and $\log K_2 = 3.27$, in water) and derivatives [43]; the lower log *K* values of **2c** (respectively, 8 and 2.83) relatively to those of benzoylhydrazine, especially for the NH group, may be due to the nearby electron-withdrawing sulfonamide that stabilizes the basic form therefore retarding the protonation process.

The second protonation step of **2c** was kinetically slow to enable a quick equilibrium achievement. In parallel, ^{1}H NMR stability studies of **2c** were conducted in 2 months, and allowed to conclude about its great hydrolytic stability for $1 < pD < 9$ (see below). The high stability of **2c** is a very relevant feature, and therefore the found kinetic problems may be due to the tautomeric equilibrium of the hydrazide moiety:

$$RCONHNH_2 \rightleftharpoons RC(OH)=NNH_2.$$

3.3.2. Zinc complexation

Potentiometric titrations of the systems Zn(II)/L (L ≡ **2b–2d**) were carried out at 1:1 and 1:2 metal to ligand molar ratios. From the curve fitting analysis, the overall complex formation constants ($\log \beta_{Zn_mH_hL_l}$) were determined and the values are depicted in Table 1. For compounds **2b** and **2c**, the Zn(II) complexation begins above pH 5 and 5.5, respectively, while for compound **2d** it begins above pH 4.5 (see Fig. 3). Once more, for compound **2b**, kinetic problems were observed in the pH range 6.5–7.4, with the need for a higher acquisition period (*ca* 15 h). The proposed equilibrium model involves always the species ZnHL, although, for pH above 7–7.5, residual amounts of the species $Zn_2H_{-4}L_2$ were also found, in the cases of Zn(II)-**2b** and Zn(II)-**2d** systems. Admitting that the protonated group is the sulfonamide ($PhOPhSO_2NH$), on the basis of the difference between the overall formation constants for the protonated complex ($\log \beta_{ZnHL}$) and the ligand protonation ($\log K_1$), a coarse evaluation of global constant for the unprotonated species ($\log \beta_{ZnL}$) with compounds **2b**, **2c** and **2d**, gave *ca* 4.6, 3.0 and 4.7, respectively. The $\log \beta_{ZnL}$ value obtained for **2b** (*ca* 4.6) gives support to a (*O*,*O*) hydroxamate coordination mode (see Fig. 4), as observed for the zinc complexes of acetohydroxamic acid (AHA) ($\log \beta_{ZnL} = 5.18$ [44] in water) or GLYHA ($\log \beta_{ZnL} = 5.38$ [45] in water); differences in the $\log \beta_{ZnL}$ values can be ascribed to the different solvents used and to the presence of a sulfonamide electron withdrawing group in **2b**.

Regarding ligand **2c**, the ZnHL species appears to have a (*N*,*O*) coordination mode established through the hydrazinic NH_2 group and the oxygen atom of the carbonyl group, according to already suggested structures in aqueous solution [46] and in solid state [47].

This hypothesis is supported by the observed downfield shift on the ^{1}H NMR signals of NH_2 and CONH due to the complexation with Zn(II) (deshielding effect of this cation): NH_2 signal shifts from 4.22 ppm (L) to 4.42 ppm (1:1 Zn/L) and 5.06 ppm (5:1 Zn/L); CO*NH* signal changes from 9.04 ppm (L) to 9.23 ppm (1:1 Zn/L) and 9.82 ppm (5:1 Zn/L). Fig. 5 shows also that the *NH*SO_2 proton of the ligand (7.85 ppm) is much less sensitive to the presence of the zinc ion than the other two labile protons; the remaining non-labile protons of the ligand are not significantly affected by the Zn(II) complexation, as expected. The integration of the peaks is consistent with the formation of only one complex species, namely under our experimental conditions.

Concerning **2d**, the ZnHL species must involve a (*N*,*O*) coordination mode involving the sulfonylhydrazide ($\log K_2 = 8.00$) and the oxygen atom of the carbonyl group, as already reported for the solid structure of zinc complexes of aroyl-hydrazones [48].

The differences between the herein estimated values of $\log \beta_{ZnL}$ for compounds **2c** (3.0) and **2d** (4.7) and the reported values for aminobenzoyl-hydrazide derivatives (6.21-6.35 in 80% (v/v) aqueous-ethanolic medium [46]), may be mostly due to the electron withdrawing nature of the neighbor sulfonamide groups present in **2c** and **2d**.

Table 1
Stepwise protonation constants (log K_i) of **2b**, **2c** and **2d** as well as the global formation constants of their Zn(II) complexes (I = 0.1 M KCl, 40% DMSO/H_2O, T = 25.0 ± 0.1 °C).

Compound	Equilibrium constant	2b	2c	2d
log K_1	[HL] / ([H][L])	10.12(1)	10.37(3)	9.74(1)
log K_2	[H_2L] / ([H][HL])	8.91(2)	8.00(5)	8.12(2)
log K_3	[H_3L] / ([H][H_2L])	–	2.83(8)	–
log β_{ZnHL}	[ZnHL] / ([Zn][H][L])	14.58(9)	12.96(4)	14.46(2)

Since the ligands under study have different acid–base behavior, comparison between their affinity towards the zinc ion is better accomplished on the basis of the corresponding pZn values at the physiological pH (pZn = −log [Zn^{2+}] under the usual conditions of micromolar concentration for the metal ion and ten-fold ligand excess). Analysis of this data shows that this set of ligands presents similar affinity for zinc (pZn ≈ 6.8). This is a particularly interesting result, since it demonstrates that, besides hydroxamates, other ZBGs, such as hydrazides or arylsulfonylhydrazides, present also good affinity for the zinc ion.

3.3.3. Hydrolytic stability

A study on the hydrolytic stability of the ligands was performed for the hydroxamate **2b** and the hydrazide **2c** derivatives. For that purpose, ^{1}H NMR spectra of the ligands in 40% DMSO-d6/D_2O (C_L ca. 10–15 mM) were recorded at different pH ranges at r.t. The samples were kept at different pH conditions and r.t. for several days. Concerning **2b**, after 2 days, there was 20% decomposition at pH ca. 1, while decomposition was irrelevant between pH ca. 4 and 9. After 1 week about 40% decomposition was observed at pH ca. 1 and 15% at pH ca. 9, while no decomposition was observed between pH 4 and 7. Regarding **2c**, no decomposition was observed from pH ca. 1 to 9 for 2 weeks. After 3 months, only 10% had decomposed at pH ca. 9, while for pH 1–7 the compound was found intact. These results confirm that hydrazides possess a greater hydrolytic stability than the hydroxamic acids.

3.4. MMP inhibition

The inhibitory profile of compounds **2–5** against MMP2 and MMP14 is presented in Table 2, together with that for two reference inhibitors. These two enzymes are considered targets against cancer, a pathology in which they have been proved to play malignant roles [6,49]. The results show that several of the new compounds inhibit the tested MMPs with IC_{50} values in the nanomolar range of concentration, while others can only reach activities in the micromolar range. As expected, the hydroxamic derivatives (**2b**, **3b**, **4b**) are stronger inhibitors (IC_{50} 0.46–4.8 nM against MMP2) than their analogues with different ZBGs (the lowest IC_{50} values are 300 nM for **3c** and 337 nM for **3a** with MMP2).

Concerning the model compounds, **2**, the order of inhibition against MMP2 follows the trend **2b** > **2a** > **2c** > **2f** > **2d** > **2 g** > **2e**, with IC_{50} values ranging from 0.46 nM to >200 μM. A quite similar inhibitory profile was observed against MMP14, although, in general, the activity is higher for MMP2 than for MMP14. The fact that most of these compounds showed inhibitory values (IC_{50}) in the micromolar range reveals that they are able to bind these enzymes at some extent, in spite of not attaining optimum values (the worst IC_{50} values were found for **2e** and **2g**, both ≥178 μM). The quite low IC_{50} values found for **2b** (0.46 and 4.0 nM with MMP2 and MMP14, respectively), are only explainable by extra interactions with the enzymes, which cannot be formed with the other analogues, (eventually, other than the zinc-binding interactions). This shall be discussed later with the docking studies. The good inhibitory activity presented by the hydrazide **2c** (IC_{50} 7.2 μM) and the arylhydrazide **2f** (41 μM) gave an important contribution to the next molecular design step, whereby these groups were selected for further conjugation with optimized molecular scaffolds to provide improved inhibitory capacities.

Table 2
Inhibitory profile (IC_{50} values[a]) of the MMPI models (**2a–2g**), the BTA-based inhibitors (**3–4**) and the reference inhibitors towards MMP2 and 14.

Compounds	X-R_1[b]	IC_{50} (μM)[a]	
		MMP2	MMP14
2a	–	0.814	4.40
2b	–	0.00046	0.0040
2c	–	7.20	33.6
2d	–	64.4	>200
2e	–	>200	190
2f	–	41.0	130
2g	–	178	>200
3a	CH_2	0.337	1.76
3b		0.0006	0.0008
3c		0.300	0.713
3d		104	>200
3n		262	441
4a	CH-(*R*)-*i*Pr	7.10	40
4b		0.0048	0.120
4c		0.660	7.10
1[c]		0.00035	0.00032
CGS2702A [3]		0.0248	0.0232
5b[d]		0.0004	0.0052
5c[d]		0.550	–
5d[d]		0.024	2.60

[a] The IC_{50} values are the average of three determinations with a standard deviation of <10%.
[b] According to the general formula for compounds **3–4** (see Fig. 2).

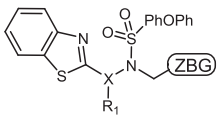

[c] Ref. [9].
[d] Illomastat derivatives (**5c–5d**) [30,50].

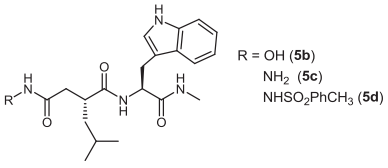

Regarding the BTA-containing compounds **3**, the trend order of the MMP inhibition is **3b** > **3c** > **3a** > **3d**, ranging from 0.6 nM to 104 μM for MMP2. The hydrazide **3c** (IC_{50} 300 nM) revealed slightly stronger inhibition than the carboxylate **3a** analog (IC_{50} 337 nM), and both showed activity increase as compared to the model compounds **2c** and **2a**. This means that the BTA group gives a positive contribution to the binding interaction of these inhibitors with the enzymes. In fact, the hydroxamate analog **3b** revealed more potent than the reference inhibitor CGS 27023A (24.8 nM). The weak inhibitory result observed for compound **3n** (260–440 μM), which bears only the arylsulfonyl and the BTA moieties, demonstrates that, alone, these two groups are not enough to accomplish a good MMP inhibition. This fact proves that the chelating groups included in compounds **3–4** are essential and should play the role of ZBG in these MMPIs. Regarding the hydroxamate **3b**, its inhibitory activity is slightly lower than for **2b**, and this must be due to a decrease of the binding interactions. Nevertheless, the low IC_{50} values (sub-nanomolar range) clearly indicate that the BTA is still strongly interacting with the enzymes. Concerning the arylsulfonylhydrazides, an unexpected reduction in the inhibitory activity was observed from **2d** to **3d** (IC_{50} of 64 and 104 μM, respectively). Apparently, in this case, the position occupied by the BTA within the enzymes is different from

those of compounds **3a**–**3c**, and the introduction of this group becomes unfavorable to the adduct stability. On the other hand, it has been shown that the arylsulfonylhydrazides, when inserted in an optimized molecule, may lead to very potent MMPIs, such as compound **5d** (IC_{50} 24 nM, see Table 2) which turned out to be an even stronger inhibitor than the hydrazide analog **5c** (550 nM). However, it is known that the type of aryl group present may considerably change the IC_{50} values of the inhibitors. Since herein we have tested only one group (4-methoxybenzene), perhaps with a different aromatic group in the arylsulfonylhydrazide (e.g. biphenyl) the results might have been different [30].

For compounds **4**, the MMP inhibition ranged from 4.8 nM to 7.1 μM with MMP2. In this series, only the carboxylate, hydroxamate and hydrazide derivatives (**4a**, **4b** and **4c**) were prepared, in order to check the inhibition sequence, which was the same as found for series **3**. The IC_{50} values observed for derivatives **4** were all higher with respect to their **3** analogues, meaning that the bulkier isopropyl spacer of compounds **4** hinders inhibition.

3.5. Molecular docking

In order to rationalize the inhibitory profiles observed for the tested compounds, in terms of molecular interactions, we decided to make use of a very versatile computational technique, which is molecular docking. For that, the 3D structure of MMP2, our target cancer-related MMP, was taken from entry 1QIB of the RCSB Protein data Bank (PDB) [25] and the ligands were docked using GOLD 4.0 software [27], following a previously validated procedure [9]. This method makes use of the known very conserved positions adopted by the carboxylic- and hydroxamic-ZBGs of MMPIs and sets their position with a scaffold-match constraint (see Experimental section for details).

Most of the compounds showed, as expected, a feature common to many arylsulfonamide-based MMPIs: the aromatic PhOPh moiety is well inserted into the hydrophobic S1′ cavity, with the sulfonyl group forming H-bonds with the backbone NH groups of Leu191 and Ala192 (MMP2 numeration). This feature is responsible for the considerable stability of the corresponding adducts, and it is, according to our expectations, based on recent outlined advantages of inserting arylsulfonamide moieties in new sets of MMPI [51]. The most potent compound studied herein is **2b** (Fig. 6a), and its docking gives support to the higher activity demonstrated by the HA-based MMPIs: they form a chelate with Zn(II), by coordinating it with both O-atoms, and they establish H-bonds with Glu404 and the Ala192 carbonyl groups. In the case of **2b**, an extra H-bond, formed between the sulfonamide NH group and the Pro423 carbonyl, provides extra stabilization to the complex formed with MMP2, thus giving support to the corresponding sub-nanomolar IC_{50} value. **2a** coordinates Zn(II) with one O-atom, and it seems to adopt a positioning quite different from that of **2b**, forming less interactions with the protein, although several H-bonds are maintained.

Regarding the compounds bearing other ZBGs, their binding conformation was not accurately confirmed in silico due to the high demands in computational tools that would be required to analyze the real coordinating mode of the Zn(II) (e.g. using quantum mechanics simulations). However, according to the docking calculations, compound **2c** seems to be able to adopt the same conformation as **2b**, with the hydrazide group chelating the metal ion via its *N*,*O*-donor atoms. The same H-bonds can be found in the docking conformation, except the one between the sulfonamide NH group and Pro423. The lack of this H-bond might explain the lower IC_{50} value displayed by **2c**. Regarding compounds **2d** and **2f** (Fig. 6b), interestingly, they seem to be able to bind the Zn(II) in a similar way as **2c**, and to adopt conformations close to this ligand, while their methoxyphenyl group lays over the S2 sub-site region, interacting with the aromatic valley His407–His413. However, even if some important H-bond interactions are maintained (namely with Glu404 and Ala192) and a new one may be formed (between the Ala194 NH and the **2d** hydrazide-SO_2 groups), the interaction of the arylsulfonamide-SO_2 with Leu191 and Ala192 has been considerably weakened, and this fact may explain the lower inhibitory potency of these compounds as compared with **2c**. Concerning the hydrazones **2e** and **2g**, they were unable to orientate the ZBG towards the Zn(II) because of steric hindrance, this being a probable major reason for their low inhibitory activity.

The docking results for the BTA-derivatives allowed understanding some of their inhibitory properties. Most of these bifunctional compounds and the model inhibitors **2** presented some similar binding interactions, namely those involving the ZBGs and the catalytic Zn^{2+}, as well as those between the $PhOPhSO_2$ moieties with the enzyme. In Fig. 7a are displayed compounds **3a**–**3c**, in which it is possible to see the BTA moiety laying over the region of His413 and Pro423, forming strong aromatic and van der Waals interaction with these residues. This fact explains the enhancement of activity from compounds **2a** and **2c** to **3a** and **3c**, respectively. On the other hand, compound **3b** does not have the ability for H-bonding to Pro423, like its parent **2b**, and the favorable interactions of the BTA moiety are not enough to compensate this energetic loss, thus explaining the reduction of inhibitory activity. Regarding **3d**, some difficulties were revealed for the fitting of the two big aromatic groups (BTA and the arylsulfonylhydrazide) in the catalytic center of MMP2, and,

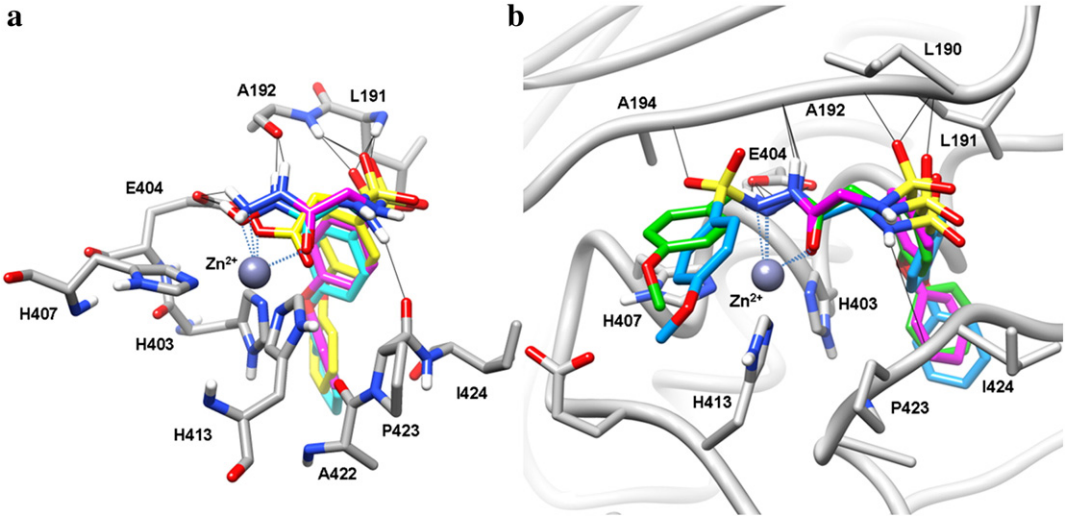

Fig. 6. Docking of compounds into MMP2: a) **2a** (yellow), **2b** (cyan), and **2c** (magenta); b) **2c** (magenta), **2d** (blue), and **2f** (green). The black solid lines represent the H-bonds.

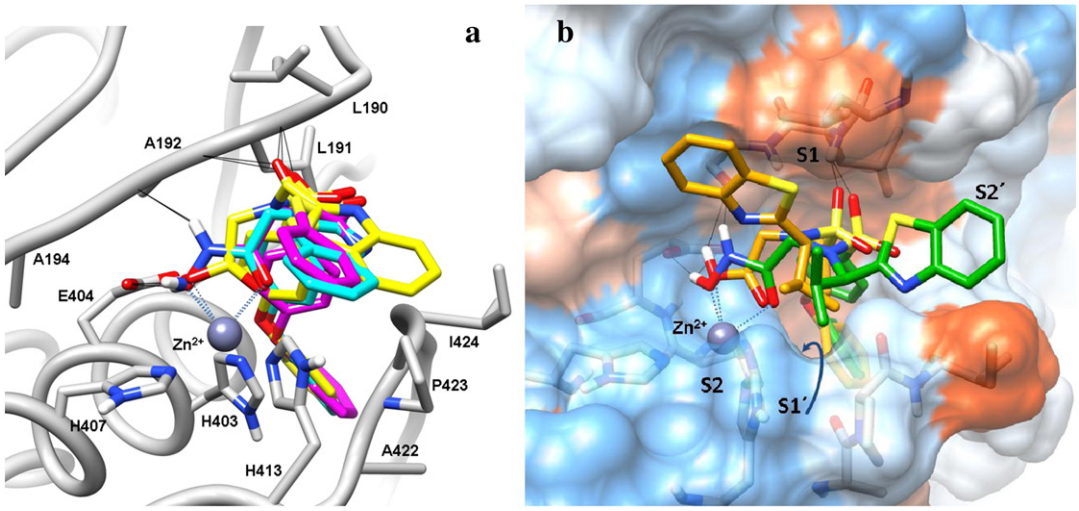

Fig. 7. Docking of compounds into MMP2: a) **3a** (yellow), **3b** (cyan), and **3c** (magenta); b) **4a** (orange) and **4b** (green). The black solid lines represent the H-bonds.

according to the docking results, this compound was not able to properly interact with Zn like its parent compound **2d**. We might anticipate that if a more flexible spacer was attached to the BTA group, probably a better fitting would also have been possible. In Fig. 7b are presented compounds **4a** and **4b**, which also form strong interactions with MMP2 (namely the Zn-binding and the H-bonds). However, for **4a**, the geometry of the BTA-spacer does not allow the best interaction of the BTA group, as for **3a** and **3b**, establishing only van der Waals contact with Leu190, on the S1 sub-site, while the isopropyl group does not apparently form any relevant interaction. On the other hand, the BTA group of **4b** is flexible enough to swing and form contacts with both Leu190 and Ile424, thus giving some stability to its adduct with MMP2, hence with a lower inhibition decrease with respect to **3a** vs. **4a**. Finally, the docking of **4c** was very similar to **4b**, and it explains the observed decrease in the inhibitory activities, when going from **3c** to **4c**, which is of the same order of magnitude as **3b** vs. **4b**.

3.6. Effect of MMPIs in tumor cell viability

A selection of MMP inhibitors (**2b**, **2c**, **3b**, **3c** and **4b**) was assessed for their anti-tumor activity. In particular, we aim to evaluate the effect of the extra-functional benzothiazole (BTA) group on the cytotoxic activity against the human epithelial ovarian carcinoma cells (A2780), using the Mosmann method [52]. The viability of the cells in the presence of the tested compounds was compared to that of control cultures to obtain the growth inhibition (%) and the corresponding IC_{50} value (Table 3 and Fig. S2). Furthermore, taking into account eventual effects of the compound lipophilicity in the cell membrane crossing ability, *clog P* was calculated for the same set of compounds (Table 3). All the tested compounds evidenced antiproliferative activity in the micromolar concentration range. However, the highest cytotoxicity was presented by the BTA-bearing hydroxamates **3b** and **4b** (IC_{50} ca. 10 μM), while the others only reached moderate (**2b**, **3c**) or low (**2c**, **3d**) cytotoxicity values. Furthermore, comparison between the activities of the analog compounds without BTA moiety (**2b** and **2c**) and those with this moiety (**3b**, **4b**, and **3c**) confirms the important contribution of the extrafunctional BTA group of these MMPIs on the enhancement of their anti-tumor activity. The increased lipophilicity associated to the BTA-based derivatization does not seem a rationale for the activity enhancement, since **3d** is the most lipophilic derivative and it presented one of the lowest activities. Interestingly, the compounds differing only on ZBG type presented some parallelism between the activity orders followed for the cell cytoxocity and the MMP inhibition (**2b** > **2c** and **3b** > **3c** > **3d**), whereas no direct correlation would be apparently expected. Although several possible explanations have been suggested for BTA-based anticancer agents (from formation of adducts with DNA to tyrosine kinase inhibition [53–55]), the mechanism responsible for the cytotoxicity of these particular bifunctional BTA-bearing MMP inhibitors against the ovarian carcinoma cells still needs further clarification.

Altogether, our results have shown that with a rational molecular design it will be possible to tune the "BTA-spacer" moiety to optimize the MMP inhibitory activity. At the same time, the BTA substituent might be varied and optimized to enhance the overall antiproliferative action against tumor cells of a new generation of MMPIs.

4. Conclusions

A new set of bifunctional matrix metalloproteinase inhibitors (MMPIs) has been developed and studied herein, aimed at improving the anti-cancer activity and decreasing drawbacks associated with the MMPIs containing hydroxamate (HA) zinc-binding groups (ZBG). As a first strategy, inspired in the pharmacophore mapping of the HAs when bound to the catalytic center of the matrix metalloproteinases (MMPs), a series of inhibitor models, bearing a set of different ZBGs (hydrazide (**2c**), arylsulfonyl- and aryl-hydrazide (**2d**, **2f**), as well as acylhydrazone (**2e** and **2g**)), have been developed and studied. Solution equilibrium studies, performed for some of those model compounds, revealed similar affinities for the Zn(II) (pZn values ca. 6.8 at pH 7.4). The inhibitory activities towards two tumor-related MMPs (MMP2 and 14, over-expressed in human ovarian tumor cells) showed that the most

Table 3
IC_{50} values (μM) for A2780 ovarian carcinoma cells after 72 h continuous treatment with the compounds, as well as cisplatin for comparison. The calculated log *P* values (*clog P*) are also depicted.

Compounds	IC_{50} (μM)	*clog P*[a]
2b	58.4 ± 15.0	0.07
2c	123 ± 20.5	0.93
3b	10.5 ± 3.2	1.58
3c	45.1 ± 8.6	2.61
3d	81.5 ± 14.5	4.23
4b	9.5 ± 4.5	2.07
Cisplatin	2.5 ± 0.3[b]	–

[a] Predicted values using QikProp program, v. 2.5, Ref. [56].
[b] Ref. [28].

potent inhibitor was of HA type (**2b**, IC_{50} 0.46 nM with MMP2), followed by the carboxylic (**2a**, 814 nM), the hydrazide (**2c**, 7.2 μM) and the arylhydrazide (**2f**, 41 μM) analogues. In a second step of our strategy to reinforce the anti-tumor activity, a selection of those models was further extra-functionalized with benzothiazole (BTA), a moiety with recognized antitumor activity. Some of the new bifunctional compounds revealed considerable MMPI activity, as compared with the model compounds, ranging from subnanomolar to micromolar concentration activity (e.g. the hydroxamate **3b**, IC_{50} 0.6 nM, and the hydrazide **3c** towards MMP2). Similarly, this BTA-derivatization lead to a great improvement on the anti-proliferative activity of a human ovarian cancer cell line (A2780). Remarkable was the fact that the bifunctional BTA-hydrazide derivatives presented considerably high activity on the MMP2 inhibition (eg. **3c**, IC_{50} 300 nM) and also on the anti-proliferation of ovarian cancer cells (IC_{50} 45 μM), besides demonstrating hydrazide resistance to hydrolysis, in opposition to the HA lability. Therefore, although further studies need to be done, this set of results suggests that some of these bi-targeting compounds may be considered as lead compounds for a new generation of MMPIs with anticancer properties although, by now, implications for therapy applications are obviously only speculative.

Abbreviations

AHA	acetohydroxamic acid
ATP	2-aminothiophenol
Boc	*tert*-butyloxycarbonyl group
BTA	benzothiazole
COSY	correlation spectroscopy
DMAP	4-dimethylaminopyridine
Dmb	2,4-dimethoxybenzyl group
EDC.HCl	1-ethyl-3-(3-dimethylaminopropyl)carbodiimide hydrochloride
FAB	fluorometric assay buffer
FBS	fetal bovine serum
GLYHA	glycine-hydroxamic acid
HA	hydroxamic acid
HSQC	heteronuclear single quantum coherence spectroscopy.
ICMHA	iminocarboxymethyl-hydroxamic acid
MMP	matrix metalloproteinase
MMPI	MMP inhibitor
MTT	3-(4,5-dimethylthiazol-2-yl)-2,5-diphenyltetrazolium bromide
NMM	*N*-methylmorpholine
PDB	protein data bank
r.t.	room temperature
TFA	trifluoroacetic acid
TLC	thin layer chromatography
T3P	propylphosphonic anhydride
ZBG	zinc-binding group

Acknowledgments

Financial support is acknowledged to the Portuguese *Fundação para a Ciência e Tecnologia* (F.C.T.), with the post-doc grant SFRH/BPD/29874/2006. The authors are grateful for financial support given by MIUR (Prin 2007, *Design, Synthesis and Bioevaluation of Activity Modulators of Metalloenzymes involved in Tumoral, Neuroinflammatory and Neurodegenerative Processes*) and to the University of Pisa for the Erasmus grant to C. A. (Lisboa04). We also thank the Portuguese NMR and MS Networks (IST-UTL Center) for providing access to their facilities. Molecular graphics and analyses were performed with the UCSF Chimera package, which is developed by the Resource for Biocomputing, Visualization, and Informatics at the University of California, San Francisco (supported by NIGMS 9P41GM103311).

Appendix A. Supplementary data

Supplementary data to this article can be found online at http://dx.doi.org/10.1016/j.jinorgbio.2013.03.003.

References

[1] M. Whittaker, C.D. Floyd, P. Brown, A.J. Gearing, Chem. Rev. 99 (1999) 2735–2776.
[2] M. Egeblad, Z. Werb, Nat. Rev. Cancer 2 (2002) 161–174.
[3] a) A.K. Sood, M.S. Fletcher, J.E. Coffin, M. Yang, E.A. Seftor, L.M. Gruman, D.M. Gershenson, M.J.C. Hendrix, Am. J. Obstet. Gynecol. 190 (2004) 899–909;
b) X. Hu, D. Li, W. Zhang, J. Zhou, B. Tang, L. Li, Arch. Gynecol. Obstet. 286 (2012) 1537–1543.
[4] H. Nagase, R. Visse, in: C.T. Supuran, J.-Y. Winum (Eds.), Drug Design of Zinc–Enzyme Inhibitors, John Wiley, NY, 2009, pp. 489–506.
[5] L.M. Coussens, B. Fingleton, L.M. Matrisian, Science 295 (2002) 2387–2392.
[6] C.M. Overall, O. Kleifeld, Nat. Rev. Cancer 6 (2006) 227–239.
[7] M. Flipo, J. Charton, A. Hocine, S. Dassonneville, B. Deprez, R.J. Deprez-Poulain, J. Med. Chem. 52 (2009) 6790–6802.
[8] A. Rossello, E. Nuti, in: C.T. Supuran, J.-Y. Winum (Eds.), Drug Design of Zinc–Enzyme Inhibitors, John Wiley, NY, 2009, pp. 549–590.
[9] S.M. Marques, E. Nuti, A. Rossello, C.T. Supuran, T. Tuccinardi, A. Martinelli, M.A. Santos, J. Med. Chem. 51 (2008) 7968–7979.
[10] J. Jacobsen, J.L. Fullagar, M.T. Miller, S.M. Cohen, J. Med. Chem. 54 (2011) 591–602.
[11] M.A. Esteves, O. Ortet, A. Capelo, C.T. Supuran, S.M. Marques, M.A. Santos, Bioorg. Med. Chem. Lett. 20 (2010) 3623–3627.
[12] S.M. Marques, T. Tuccinardi, A. Martinelli, S. Santamaria, E. Nuti, A. Rossello, V. André, M.A. Santos, J. Med. Chem. 54 (2011) 8289–8298.
[13] P.S. Yadav, Devprakash, G.P. Senthilkumar, Int. J. Pharm. Sci. Drug Res. 3 (2011) 1–7.
[14] S. Aiello, G. Wells, E.L. Stone, H. Kadri, R. Bazzi, D.R. Bell, M.F. Stevens, C.S. Matthews, T.D. Bradshaw, A.D. Westwell, J. Med. Chem. 51 (2008) 5135–5139.
[15] M. Wang, K.D. Miller, G.W. Sledge, G.D. Hutchins, Q.-H. Zheng, Bioorg. Med. Chem. 14 (2006) 8599–8607.
[16] W.L.F. Armarego, D.D. Perrin, Purification of Laboratory Chemicals, 4th ed. Butterworth-Heinemann, Oxford, 1999.
[17] M.A. Santos, S.M. Marques, T. Tuccinardi, P. Carelli, L. Panelli, A. Rossello, Bioorg. Med. Chem. 14 (2006) 7539–7550.
[18] F.J.C. Rossotti, H. Rossotti, J. Chem. Ed. 42 (1965) 375–378.
[19] P. Gans, A. Sabatini, A. Vacca, Talanta 43 (1996) 1739–1753.
[20] C.G. Knight, F. Willenbrock, G. Murphy, FEBS Lett. 296 (1992) 263–266.
[21] SoftMax Pro 4.7.1 by Molecular Devices.
[22] GraFit version 4 by Erithecus Software.
[23] Maestro, version 7.5, Schrödinger Inc., Portland, OR, 2005.
[24] Macromodel, version 8.5, Schrödinger Inc., Portland, OR, 1999.
[25] H.M. Berman, J. Westbrook, Z. Feng, G. Gilliland, T.N. Bhat, H. Weissig, I.N. Shindyalov, P.E. Bourne, Nucleic Acids Res. 28 (2000) 235–242.
[26] E.F. Pettersen, T.D. Goddard, C.C. Huang, G.S. Couch, D.M. Greenblatt, E.C. Meng, T.E. Ferrin, J. Comput. Chem. 25 (2004) 1605–1612.
[27] G. Jones, P. Willett, R.C. Glen, A.R. Leach, R. Taylor, J. Mol. Biol. 267 (1997) 727–748.
[28] C. Francisco, S. Gama, F. Mendes, F. Marques, I.C. Santos, A. Paulo, I. Santos, J. Coimbra, E. Gabano, M. Ravera, Dalton Trans. 40 (2011) 5781–5792.
[29] F. Augé, W. Hornebeck, J.-Y. Laronze, Crit. Rev. Oncol./Hematol. 49 (2004) 277–282.
[30] G. LeDour, G. Moroy, M. Rouffet, E. Bourguet, D. Guillaume, M. Decarme, H. ElMourabit, F. Augé, A.J.P. Alix, J.-Y. Laronze, G. Bellon, W. Hornebeck, J. Sapi, Bioorg. Med. Chem. 16 (2008) 8745–8759.
[31] M. Rouffet, C. Denhez, E. Bourguet, F. Bohr, D. Guillaume, Org. Biomol. Chem. 7 (2009) 3817–3825.
[32] T. Mistri, M. Dolai, D. Chakraborty, A.R. Khuda-Bukhsh, K.K. Das, M. Ali, Org. Biomol. Chem. 10 (2012) 2380–2384.
[33] A.A.R. Despaigne, J.G. Da Silva, A.C.M. Do Carmo, O.E. Piro, E.E. Castellano, H. Beraldo, J. Mol. Struct. 920 (2009) 97–102.
[34] M.D. Altıntop, A. Özdemir, G. Turan-Zitouni, S. Ilgın, Ö. Atlı, G. İşcan, Z.A. Kaplancıklı, Eur. J. Med. Chem. 58 (2012) 299–307.
[35] D. Perdicchia, E. Licandro, S. Maiorana, C. Baldoli, C. Giannini, Tetrahedron 59 (2003) 7733–7742.
[36] Archimica, http://www.archimica.com/pdf/archimica_t3p_brochure.pdf, November 2012.
[37] S. Chaves, S.M. Marques, A. Cachudo, M.A. Esteves, M.A. Santos, Eur. J. Inorg. Chem. (2006) 3853–3860.
[38] C. Hansch, A. Kurup, R. Garg, H. Gao, Chem. Rev. 101 (2001) 619–672.
[39] R. Karlicek, J. Majer, Collect. Czechoslov. Chem. Commun. 37 (1972) 151–170.
[40] R. Karlicek, M. Polasek, Collect. Czechoslov. Chem. Commun. 52 (1987) 592–601.
[41] F. Milletti, L. Storchi, L. Goracci, S. Bendels, B. Wagner, M. Kansy, G. Cruciani, Eur. J. Med. Chem. 45 (2010) 4270–4279.
[42] L.G. Chekanova, A.V. Radushev, A.E. Lesnov, E.A. Sazonova, Russ. J. Gen. Chem. 72 (2002) 1233–1237.
[43] K. Nagano, H. Tsukahara, H. Kinoshita, Z. Tamura, Chem. Pharm. Bull. 11 (1963) 797–805.
[44] E. Farkas, D. Brown, R. Cittaro, W.H. Glass, J. Chem. Soc. Dalton Trans. (1993) 2803–2807.
[45] E.B. Paniago, S. Carvalho, Inorg. Chim. Acta 136 (1987) 159–163.
[46] M.G. Abd El Wahed, S. Abd El Wanees, M. El Gamel, S. Abd El Haleem, J. Serb. Chem. Soc. 69 (2004) 255–264.
[47] F. Bottomley, Q. Rev. Chem. Soc. 24 (1970) 617–638.

[48] N. Galic, M. Rubcic, K. Magdic, M. Cindric, V. Tomisic, Inorg. Chim. Acta 366 (2011) 98–104.
[49] J. Decock, S. Thirkettle, L. Wagstaff, D.R. Edwards, J. Cell. Mol. Med. 15 (2011) 1254–1265.
[50] F. Augé, W. Hornebeck, M. Decarme, J.-Y. Laronze, Bioorg. Med. Chem. Lett. 13 (2003) 1783–1786.
[51] E. Nuti, T. Tuccinardi, A. Rossello, Curr. Pharm. Des. 13 (2007) 2087–2100.
[52] T. Mosmann, J. Immunol. Methods 65 (1983) 55–63.
[53] T.D. Bradshaw, A.D. Westwell, Curr. Med. Chem. 11 (2004) 1009–1021.
[54] C.G. Mortimer, G. Wells, J.P. Crochard, E.L. Stone, T.D. Bradshaw, M. Stevens, A.D. Westwell, J. Med. Chem. 49 (2006) 179–185.
[55] M.N. Noolvi, H.M. Patel, M. Kaur, Eur. J. Med. Chem. 54 (2012) 47–462.
[56] QikProp, version 2.5, Schrödinger, LLC, New York, NY, 2005.